

TERM PROJECT REPORT

On

MICROCHANNEL HEAT EXCHANGER

Submitted in partial fulfillment towards the degree of

BACHELOR OF TECHNOLOGY

in

MECHANICAL ENGINEERING

Prepared by

JANI PAL S. MH033(17MHUOS064)

LAKDAWALA SMIT M. MH043(17MHUBS033)

LANGALIA RIA M. MH044(17MHUOS051)



**DEPARTMENT OF MECHANICAL ENGINEERING
FACULTY OF TECHNOLOGY DHARMSINH DESAI
UNIVERSITY, NADIAD**

NOVEMBER 2020

BONAFIDE CERTIFICATE

Certified that the term work project report titled “**MICROCHANNEL HEAT EXCHANGER**” is the bonafide work of **JANI PAL(17MHUOS064), LAKDAWALA SMIT(17MHUBS033) AND RIA LANGALIA(17MHUOS051) , Bachelor of Technology in Mechanical Engineering, Semester VII, (2020-2021)** who carried out the term project under our supervision.

ABSTRACT

DESIGN AND EXPERIMENTAL INVESTIGATION OF A MICROCHANNEL HEAT EXCHANGER

Due to the high performance of electronic components, the heat generation is increasing dramatically. Heat dissipation becomes a significant issue in efficiency promotion and stable operation. Microchannel are of current interest for use in heat exchangers where very high heat transfer performance is desired. Microchannel provide high heat transfer coefficients because of their small hydraulic diameters. In this study, the design and experimental investigation of fluid flow and heat transfer in a microchannel heat exchanger is conducted. Water and air are used as the working fluids and flowed through microchannel. The heat exchanger has been designed with 6 rows of microchannel for water flow and 7 rows of microchannel for forced flow of air. The heights of the microchannel are 4 mm and 10 mm respectively for water and air flows.

ACKNOWLEDGEMENT

This is a project report on “**MICROCHANNEL HEAT EXCHANGER**” We are very thankful to our project guide Prof. MITESH N PRAJAPATI, Department of Mechanical engineering, DHARMSINH DESAI UNIVERSITY, NADIAD for his invaluable guidance and assistance. We also thank him for giving this opportunity to explore about the microchannel heat exchanger and its application in various engineering field.

Date:

PAL S JANI (17MHUOS064)
SMIT M LAKDAWALA (17MHUBS033)
RIA M LANGALIA (17MHUOS051)

TABLE OF CONTENTS

Sr No.	Description	Page No.
1.	Abstract	1
2.	Acknowledgement	2
3.	Table of Contents	3
4.	Chapter 1: Introduction	4-21
	1.1 Heat Exchanger 1.2 Miniaturization and Microchannel Concepts 1.3 Electronics cooling technology 1.4 Motivation 1.5 Present Study	
5.	Chapter 2: Literature Survey	22-30
6.	Chapter 3: Theory of heat Exchanger	31-44
	3.1 Heat transfer Analysis 3.2 Overall Thermal Coefficient, UA 3.3 Fin Efficiency 3.4 Heat Exchanger Effectiveness and NTU 3.5 Pressure Drop 3.6 Heat Exchanger Coefficient 3.7 Geometrical Properties	
7.	Chapter 4: Sample Calculation	45-52
8.	Chapter 5: Drawing of Microchannel Heat Exchanger	53-65
9.	Chapter 6: Advantages and Disadvantages	66-67
10.	Chapter 7: Applications	68-69

CHAPTER 1

INTRODUCTION

This introductory chapter aims at presenting the need of understanding heat exchangers with microchannel flow and heat transfer from an electronics cooling point of view, in conjunction with the global trends in cooling technologies and the requirements of the national defense industry.

1.1 Heat Exchanger

A heat exchanger is a device that is used to transfer thermal energy between two or more fluids, between a solid surface and a fluid, or between solid particles and a fluid, at different temperatures and in thermal contact. Typical applications include heating or cooling of a fluid stream of concern and evaporation or condensation of single or multi component fluid stream.

Heat exchangers are used in a wide variety of applications. These involve power production, process, chemical and food industries, electronics, environmental production engineering, waste heat recovery, manufacturing industry, air conditioning, refrigeration and space applications. Over the past quarter century, the importance of heat exchanger has increased immensely from the viewpoint of energy conservation, conversion, recovery and successful implementation of new energy sources. Heat exchangers constitute a multibillion dollar industry in the United States alone and there are over 300 companies engaged in the manufacture of a wide array of heat exchangers.

Heat exchangers can be classified in many different ways; for example, according to transfer processes, number of fluids and heat transfer mechanism,

construction type and flow arrangements. Another arbitrary classification can be made, based on the heat transfer surface area/volume ratio into compact and non-compact heat exchangers.

A crossflow exchanger is a heat exchanger in which the two fluids flow in directions normal to each other. This is one of the most common flow arrangements used for extended surface heat exchangers because it greatly simplifies the header design at the entrance and exit of each fluid. Thermodynamically, the effectiveness for the crossflow exchanger falls in between that for the counter flow and parallel flow arrangements.

A fluid stream is considered unmixed when it passes through individual flow channels or tubes with no fluid mixing between adjacent flow channels. Fig. 1.1 shows a typical plate-fin unmixed-unmixed crossflow heat exchanger. As seen in Fig. 1.2, outlet temperatures of the fluids in a plate-fin unmixed-unmixed crossflow heat exchanger are not constant and show variations from one corner to the other corner of heat exchanger.

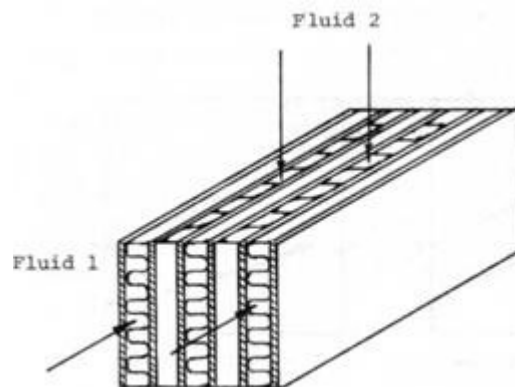


Figure 1.1: A plate-fin unmixed-unmixed crossflow heat exchanger

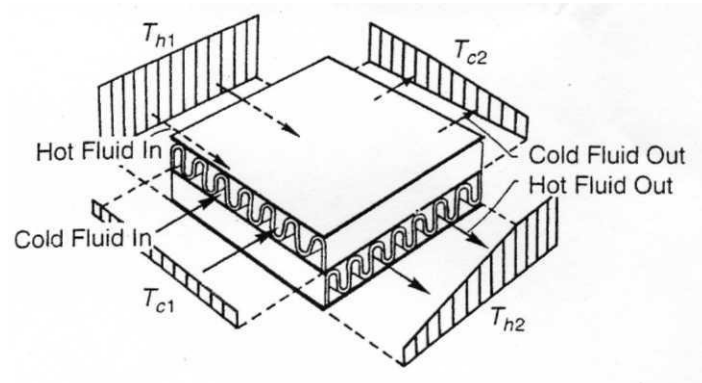


Figure 1.2: Temperature distribution in an unmixed-unmixed crossflow heat exchanger

The heat transfer surface is a surface of the exchanger core that is in direct contact with fluids and through which heat is transferred by conduction. That portion of the surface that is in direct contact with both the hot and cold fluids and transfer heat between them is referred to as the primary or direct surface. To increase the heat transfer area, appendages may be intimately connected to the primary surface to provide an extended, secondary or indirect surface. These extended surface elements are referred to as fins. Thus, heat is conducted through the fin and convected from the fin to the surrounding fluid, or vice versa, depending on whether the fin is being cooled or heated. As a result, the addition of fins to the primary surface reduces the thermal resistances on that side and thereby increases the total heat transfer from the surface for the same temperature difference. Fins may form flow passages for the individual fluids, but do not separate the two fluids of the exchanger. These secondary surface or fins may also be introduced primarily for structural strength purpose or to provide thorough mixing of a highly viscous liquid.

Fins are die or roll formed and are attached to the plates by brazing, soldering, adhesive bonding, welding, mechanical fit or extrusion. Plate fins are categorized as (1) plain and straight fins, such as plain triangular and rectangular fins, (2) plain but wavy fins (wavy in the main fluid flow direction) and (3)

interrupted fins, such as offset strip, louver, perforated and pin fins. Fin geometries for plate-fin heat exchangers are presented in Fig. 1.3.

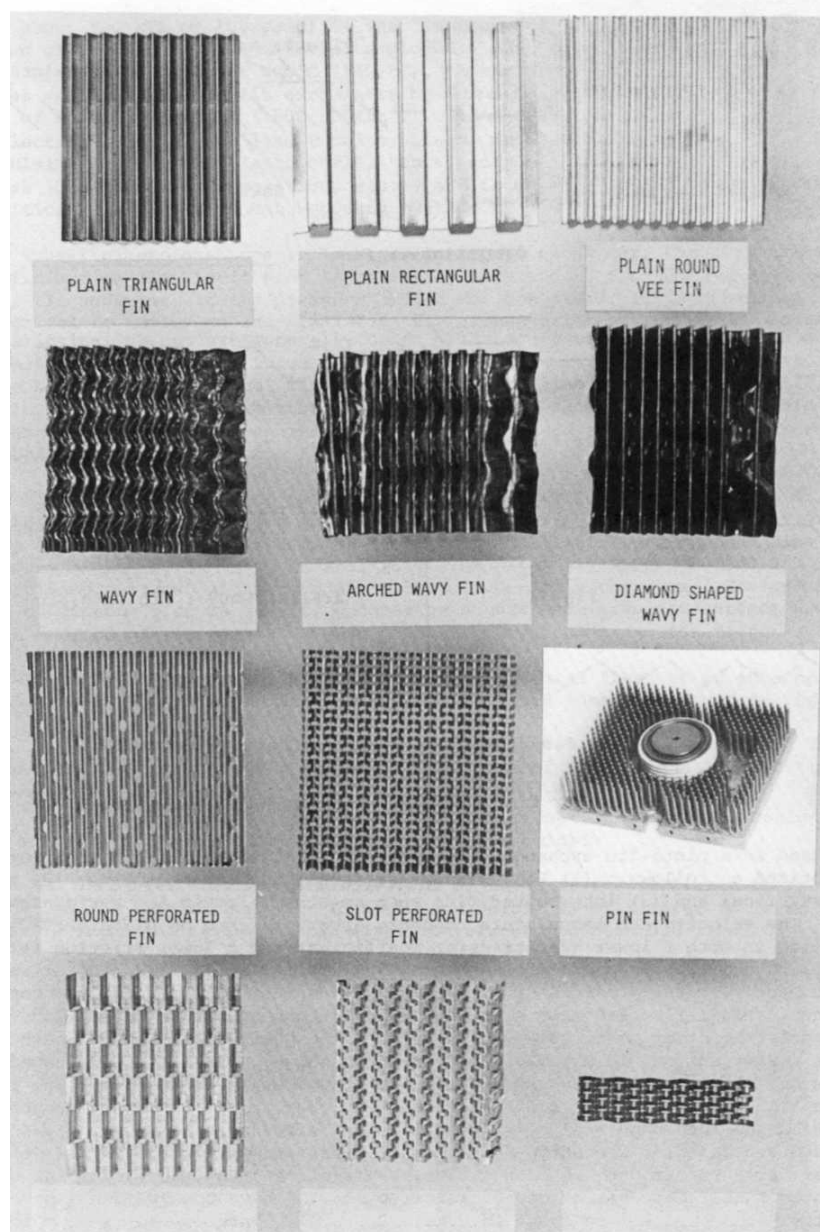


Figure 1.3: Plain, wavy and interrupted fin geometries for plate fin heat exchangers

Plate fin heat exchangers are designed to pack a high heat transfer capacity into a small volume. They consist of a series of flat plates employing a sandwich-

type construction. The space between the parting sheets is filled with fins that are stamped and folded in an accordion pattern. The fins are usually bended to the parting sheets by brazing. Some typical construction examples of plate-fin heat exchangers are shown in Fig. 1.4.

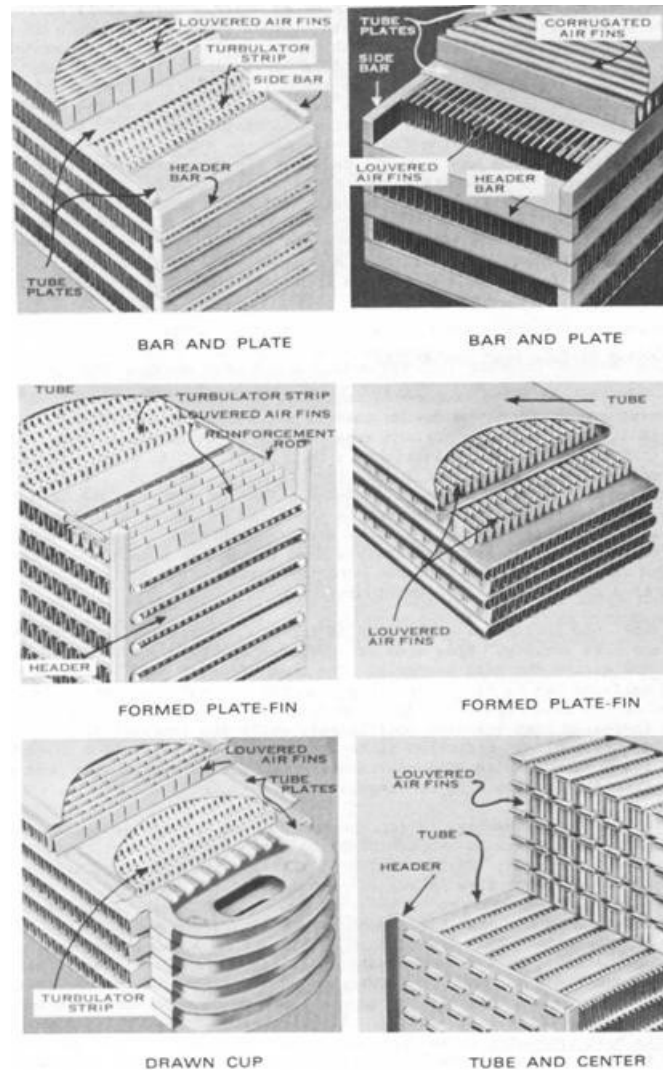


Figure 1.4: Plate fin heat exchangers [2]

1.2 Miniaturization and Microchannel Concepts

The concept of miniaturization may be said to form the basis of a relatively young field of technology, *Microelectromechanical Systems* (MEMS). When Richard P. Feynman referred to his anticipation of a trend towards miniaturization in his talk titled “There’s Plenty of Room at the Bottom”, delivered at the annual meeting of the American Physical Society in 1959, he made a striking remark: “In the year 2000, when they look back at this age, they will wonder why it was not until the year 1960 that anybody began to seriously move in this direction.”.

It was not until two decades after Feynman’s famous speech that Tuckerman and Pease first made use of miniaturization for the purposes of heat removal, within the scope of a Ph.D. study in 1981. Their publication titled “High Performance Heat Sinking for VLSI” is credited as the first study on microchannel heat transfer. Their pioneering work has motivated many researchers to focus on the topic and microchannel flow has been recognized as a high performance heat removal tool ever since. Presently, modeling and experimental investigation of microchannel flow and heat transfer are rapidly maturing, although conflicts among researchers as to how microscale flows should be modeled and discrepancies between experimental results remain.

As is evident from the diversity of application areas, the study of flow and heat transfer in microchannel is very important for the technology of today and the near future, as developments are following the trend of miniaturization in all fields.

Before proceeding with microchannel flow and heat transfer, it is appropriate to introduce a definition for the term “microchannel”. The scope of the term is among the topics of debate between researchers in the field. Mehendale et al. used the following classification based on manufacturing techniques

required to obtain various ranges of channel dimensions, “ C_D ”, being the smallest channel dimension:

$1\ \mu\text{m} < C_D < 100\ \mu\text{m}$: Microchannel
$100\ \mu\text{m} < C_D < 1\ \text{mm}$: Minichannel
$1\ \text{mm} < C_D < 6\ \text{mm}$: Compact passages
$6\ \text{mm} < C_D$: Conventional passages

Kandlikar and Grande adopted a different classification based on the rarefaction effect of gases in various ranges of channel dimensions, “ C_D ” being the smallest channel dimension:

$1\ \mu\text{m} < C_D < 10\ \mu\text{m}$: Transitional Microchannel
$10\ \mu\text{m} < C_D < 200\ \mu\text{m}$: Microchannel
$200\ \mu\text{m} < C_D < 3\ \text{mm}$: Minichannels
$3\ \text{mm} < C_D$: Conventional passages

A simpler classification was proposed by Obot based on the hydraulic diameter rather than the smallest channel dimension. Obot classified channels of hydraulic diameter under 1 mm ($D_h < 1\ \text{mm}$) as microchannel, which was also adopted by many other researchers such as Bahrami and Bayraktar. This definition is considered to be more appropriate for the purposes of this thesis as the classification proposed by Kandlikar and Grande is based on the behavior of gas flows, which is partially outside the scope of this study, and the classification proposed by Mehendale is based on manufacturing processes which are expected to change and/or improve in the future. The definition adopted by Obot is more convenient as it is based on the channel geometry alone and that it makes use of the hydraulic diameter concept, which is the primary representative dimension for internal flow geometry of the heat exchanger.

In the last few decades, new frontiers have been opened up by advances in our ability to produce microscale devices and systems. The numerous advantages that can be realized by constructing devices with microscale features have, in many cases, been exploited without a complete understanding of the way the miniaturized geometry alters the physical processes. Microchannel are used in a variety of devices incorporating single-phase liquid flow. Their extremely high heat transfer capability is the primary point of interest of microchannel for this thesis. Besides heat related applications, microscale fluid flow also finds important applications in MEMS. Micro ducts are used in infrared detectors, diode lasers, and miniature gas chromatographs; micropumps are used for inkjet printing, environmental testing, and electronics cooling; microturbines are being developed as miniature energy generators and microvalves. Chemical and biological applications such as microreactors and lab-on-a-chip devices are also many.

Microelectronic devices, which include a variety of applications such as PCs, servers, laser diodes and Rf devices are constantly pushing the heat flux density requirements to higher levels. What seemed to be an impossibly high limit of 200 W/cm^2 of heat dissipation in 1993 now seems to be a feasible target. The new challenge for the coming decade is on the order of $600\text{-}1000 \text{ W/cm}^2$. The available temperature differences are becoming smaller, and in some cases as low as only a few $^{\circ}\text{C}$. These high levels of heat dissipation require a dramatic reduction in the channel dimensions, matched with suitable coolant loop systems to facilitate the fluid movement away from the heat source.

The higher volumetric heat transfer densities require advanced manufacturing techniques and lead to more complex manifold designs. During the past two decades dramatic advances have been made in microfabrication techniques. Many of the same manufacturing techniques developed for the fabrication of electronic circuits are being used for the fabrication of compact heat exchangers. A systems perspective will be taken,

which involves transferring the heat generated in the electronic components through a path involving multiple media, leading to its ultimate rejection. Since this rejection is to ambient air for most ground based electronic equipment, liquid cooling schemes require a remote liquid to air heat exchanger, whose size and efficiency ultimately determine the size of the overall cooling systems. Capabilities and characteristics of micro fabrication play a key role in the development of such devices.

1.3 Electronics Cooling Technologies

Following the invention of the chip, methods for cooling of electronics have improved and sophisticated at an ever increasing pace in conjunction with the rapid development of the electronics industry. The importance of cooling for electronic components is that high temperatures not only decrease their lifetime by accelerating failure mechanisms in materials, but they also reduce the overall reliability of the assembly by accelerating failure mechanisms in connections and interfaces. The evident trend in the development of integrated circuits is that the sizes are getting smaller while the heat dissipation quantities are getting larger. To meet the rapidly rising heat densities, methods of thermal engineering applied to the cooling of electronics have evolved from primitive, passive structures to advanced systems. The power dissipation trend of INTEL processor chips, shown in Fig. 1.5, is representative of the silicon industry in general.

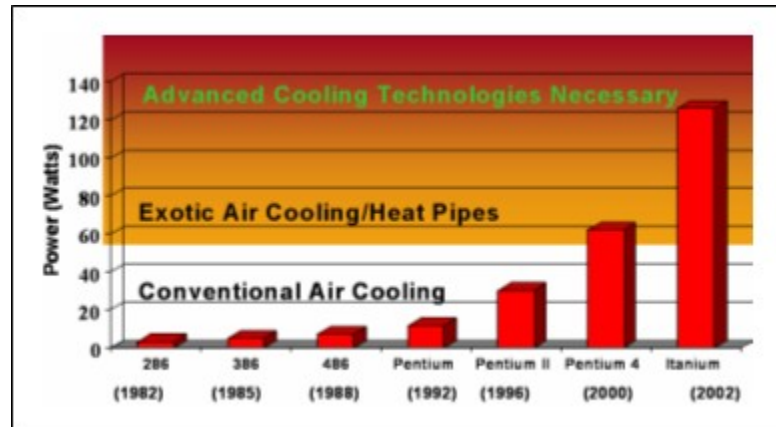


Figure 1.5: Trends in increasing power density and categorization of cooling methods employed by INTEL

The categorization of cooling methods employed by INTEL given in the figure above shows that conventional cooling methods have become insufficient by the year 2000. Conventional air cooling methods refer to making use of natural or forced convection together with heat spreaders or heat sinks. As long as the heat dissipation of the chips to be cooled is moderate, it is preferable to use a simple heat sink design that can provide adequate cooling with natural convection. For higher heat fluxes, natural convection is not sufficient and fans must be used to obtain higher heat removal rates associated with forced convection.

When conventional air cooling methods do not suffice, enhanced cooling tools such as fan-heat sink assemblies or heat pipes must be used. Fan-heat sink assemblies are commonly used in personal computers to cool high performance processors, while heat pipes are commonly used in laptop computers where space is a major limitation. Fan-heat sink assemblies are, in fact, an extension of forced cooling methods where the heat sink is designed to achieve maximum cooling performance with the air flow due to the fan attached to it. Heat pipes, on the other hand, are structures that attain extraordinarily high thermal conductivity, enabling the heat dissipated by the chips to be carried effectively to an appropriate location for cooling. Fig. 1.6 shows a heat-sink assembly and various heat pipe configurations.



Figure 1.6: A heat sink-fan assembly (left) and various heat pipe configurations (right)

When the limits of extended air cooling methods fall short of accommodating the rising heat densities to be cooled, advanced cooling technologies must be employed to achieve the high cooling performance required. The first milestone in advanced cooling is to utilize a coolant liquid instead of air. The heat removal capacity of liquids (e.g. water) is much higher compared to that of air; however, use of a liquid cooling system involves major changes in design compared to air cooling. To avoid damage to the electronics, the coolant must be totally isolated. A heat exchanger must be employed to serve as a medium of heat exchange between the coolant and the surrounding atmosphere. A pump must be used in place of the fan, heat sinks must be replaced by cold plates, or liquid cooled heat sinks, to generate a heat path between the chip and the coolant. A schematic representative of liquid cooling system is given in Fig. 1.7.

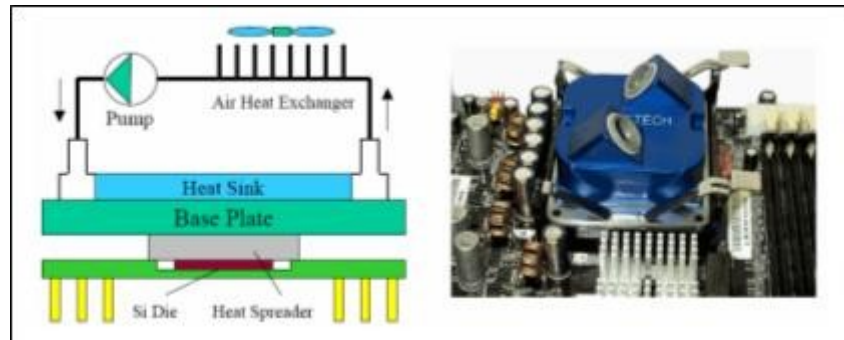


Figure 1.7: Liquid cooling system schematics (left) and example of a liquid cooled heat sink mounted on a PCB

The cooling capabilities of liquid systems are wide ranging, depending on the coolant used, the performance of the heat exchanger, the pumping power, and the thermal interface between the heat source and the coolant. Conventional liquid cooling utilizes simple liquid heat sink geometries, commonly of rectangular cross section. The cooling method is characterized by the geometry of the heat sink. The cooling capacity of the system increases as the channel size decreases, leading to the categorization of "conventional liquid cooling", "minichannel liquid cooling", and "microchannel liquid cooling". A schematic view of a liquid heat sink is shown in Fig.1.8 and also in same figure minichannel and microchannel heat sink are presented.



Figure 1.8: Schematics of liquid heat sink (left), minichannel heat sink (center), and microchannel heat sink (right)

Liquid cooling by means of conventional, minichannel, or microchannel liquid heat sinks is appropriate for the cooling of most high heat flux applications.

Many supercomputers of recent years employ microchannel liquid cooling, while microchannel liquid cooling is used most commonly in military radar applications.

In certain applications, where highly localized heat sources cannot be cooled sufficiently by channel cooling, spray cooling is employed. In this method, an atomizer (or nozzle) converts the liquid flow into a spray that impinges directly on the surface to be cooled. Dielectric coolants are used to avoid damage to the electronics. Because the coolant and heat source are brought into direct contact, the thermal path is more effective and higher cooling capacities may be achieved. Spray cooling may be designed to cool local hot spots in a system using a few nozzles, or to cool larger areas using a set of nozzles. Fig. 1.9 shows good examples of localized spray cooling and system level spray cooling.

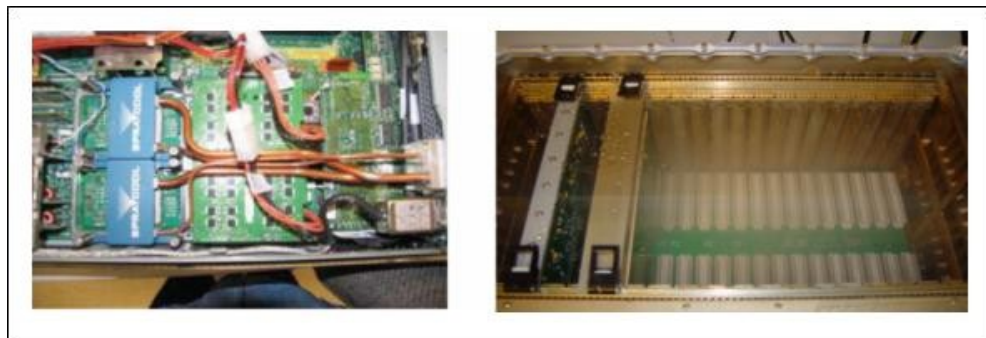


Figure 1.9: Localized spray cooling (left) and system level spray cooling (right)

A final method worth mentioning among advanced cooling technologies is thermoelectric cooling. The Peltier effect, achieved by using a series of P and N type semiconductors, causes a finite temperature difference between the two surfaces of a thermoelectric cooler when a voltage is applied. The cold side of the thermoelectric cooler is attached to the surface to be cooled, while the hot side must be cooled by another cooling system (such as a heat sink and a fan) to achieve as low a temperature as possible at the heat source. The temperature difference between the cold side and hot side of high performance thermoelectric

coolers may exceed 100°C . In this way, very low temperatures at the heat source may be obtained. The drawback of this technique is that yet another cooling method must be employed for the hot side, and the electric power requirements of thermoelectric modules are high. Thermoelectric cooling and modules are schematically shown in Fig.1.10.

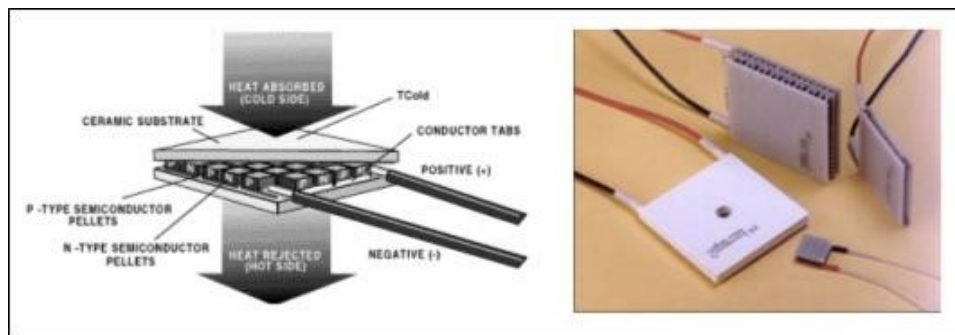


Figure 1.10: Schematic representation of thermoelectric cooling (left), thermoelectric modules (right)

1.4 Motivation

The requirements of electronics cooling are much more critical in military electronic applications when compared to commercial applications such as personal computers, laptops and communication equipment's. This is due to two reasons in conjunction. Firstly, the heat dissipation rates in military applications are usually higher; and secondly, military electronics is required to function reliably in harsh environments. The typical operating temperature specification for military equipment is the $-30^{\circ}\text{C} / +55^{\circ}\text{C}$ range and this range is being extended nowadays, i.e. the lower bound is approaching to -40°C and the upper bound is becoming $+60^{\circ}\text{C}$. Usually, the lower bound causes no problems in terms of functionality or reliability. There are, however, occasional cases in which the system must be heated to a particular temperature before beginning operation. In such instances, a heater must be employed, which is a relatively simple design consideration. It is the upper bound of $+55^{\circ}\text{C}$ that challenges the thermal engineer

in the design of thermal management systems for military electronics. Although upper limits given by manufacturers for the operating temperature of some electronic components rate as high as +150 °C, it is desirable to keep the surfaces of most components under the +85 °C level. For integrated circuits, and many other electronic components, the heat dissipated by the component causes a significant temperature rise. When heat fluxes are large, that is, when large amounts of heat are dissipated by small components, such as in high performance chips, the temperature rise of the component may be as high as 20 °C or higher.

Cooling strategies for electronic components that are to comply with military operational specifications must be designed to keep the temperature rise of the component very small. The methods of cooling required at the component level may vary from conventional air cooling to advanced cooling methods such as microchannel liquid cooling and spray cooling. The selection of the cooling method is primarily based on the maximum heat flux associated with the device or component of interest. For military applications, it is common practice to employ conventional liquid cooling for heat fluxes in the order of tens of W/cm². When the maximum heat flux to be cooled approaches or exceeds 100 W/cm², microchannel liquid cooling becomes necessary. Such high heat fluxes are frequently encountered in the microwave modules of phased array radars in military applications. A systems perspective will be taken, which involves transferring the heat generated in the electronic components through a path involving multiple media, leading to its ultimate rejection. Since this rejection is to ambient air for most ground based electronic equipment, liquid cooling schemes require a remote liquid to air heat exchanger, whose size and efficiency ultimately determine the size of the overall cooling systems. Capabilities and characteristics of the heat exchanger play a key role in cooling of electronic equipment's. Employing smaller channel dimensions in the heat exchanger results in higher heat transfer performance, although it is accompanied by a higher volumetric pressure drop per unit length. The higher volumetric heat transfer densities require advanced manufacturing techniques such as brazing and lead to more complex

designs. Because of above mentioned reasons, a brazed microchannel heat exchanger becomes the most suitable solution for military applications, which necessitate high heat removal capabilities.

1.5 Present Study

This study focuses on the experimental investigation of a microchannel heat exchanger designed for liquid cooling systems in high performance radar cooling applications. The primary aim of the work is to determine the limits of the heat removal capability of the microchannel heat exchanger, which will be used in liquid cooling systems of radar applications. The goal is to be able to cool the liquid used in systems (e.g. water).

The secondary aim of this work is to design a national microchannel heat exchanger and to manufacture with national sources. In military applications one of the most critical aims is to lessen the dependence of our country to foreign countries. By means of this study one product will not be need importing.

The other aim of this work is to gain the capability of flexibility in geometrical dimensions of the heat exchanger. Importing the product on the shelf restricts the designer and also the system in geometrical shape, dimensions, construction type, fluid type and etc. which are defined by the firms. After this study, we are able to determine the fin heights or length of the dimension and the other dimensions which the national system necessitates. In general, the ready-made product is either larger in volume or less efficient for the systems. This experience in design, and production of a microchannel heat exchanger will result in smaller and lighter liquid cooling systems in aerospace and defense industries. This experimental study will ensure that in spite of the rising heat fluxes, heat removal capacity of the system can be adjusted by altering the fin dimensions or fin type. By means of designing and producing an original microchannel heat exchanger, mounting

details of the heat exchanger will not be criteria for choosing or designing the systems. Moreover, time consumed to import a heat exchanger will decrease dramatically and also the response time to the change of design which is in nature of military projects will fall down and all these drops and flexibility result in saving money.

The starting point of this study is that if a design of the liquid cooling systems in military projects is possible, the product, the microchannel heat exchanger, to be used in this system can be also designed and national microchannel heat exchanger can be produced.

CHAPTER 2

LITERATURE SURVEY

The following is a review of the research that has been completed especially on microchannel heat exchangers (μ HEX) over the last decade. The literature survey is arranged according to similarity to the work done in this thesis.

In one of the recent studies by Al-Nmir et al, an investigation of the hydrodynamic and thermal behavior of the flow in parallel plate μ HEX is performed numerically, by adopting a combination of both the continuum approach and the possibility of slip at the boundaries. In their work, both viscous dissipation and internal heat generation were neglected. Fluent analysis was made based on solving continuum and slip boundary condition equations. The flows were assumed as laminar, two dimensional, steady and incompressible with constant thermo-physical properties and without a heat source/sink. Effects of different parameters; such as, Knudsen number (Kn), heat capacity ratio (Cr), effectiveness (ϵ), and number of transfer units (NTU) were examined. The study showed that both the velocity slip and the temperature jump at the walls increase with increasing Kn due to the flow not being completely aware of the presence of the wall as a result of the relatively low number of collisions between the fluid molecules. The increase of the slip conditions reduces the frictional resistance of the wall against the flow, and under the same pressure gradient, pumping force leads to that the fluid flows much more in the heat exchanger. It was reported that increasing Kn leads to an increase in the temperature at the heat exchanger wall. On the other hand, at low values of Kn, the NTU increases with increasing Cr, but at high values of Kn the NTU decreases with increasing Cr. With regard to the

effect of Cr on ϵ , it was found that increasing Cr leads to a reduction in ϵ for all Kn .

Very recently, Mathew and Hegab theoretically analyzed the thermal performance of parallel flow μ HEX subjected to constant external heat transfer [20]. The equations for predicting the axial temperatures as well as the effectiveness of the fluids of the μ HEX operating under laminar flow conditions were developed. In addition, an equation for determining the heat transfer between the fluids was formulated. Mathew and Hegab developed this particular model in such a way that it can be used for a parallel flow with either balanced or unbalanced flow (i.e. heat capacities of two fluids are equal or not) and also it enables to calculate the temperature of the fluids at any axial location. Moreover, the model can be used when the individual fluids are subjected to either equal or unequal amounts of external heat transfer. On the other hand, the model is limited to microchannel flow applications in which the working fluids are incompressible, single phase, maintaining no-slip wall conditions, and do not exhibit any rarefaction effects. The last restriction results in a restriction on the lower limit of the microchannel diameter. For example, if air is used, the minimum hydraulic diameter must be 68 nm which is the mean free path of air. In this paper, under unbalanced flow conditions, it was stated that the effectiveness of the fluids depend on the fluid with the lowest heat capacity, it is greatest when the hot fluid has the lowest heat capacity. At a given NTU, the reduction in heat capacity ratio improved the effectiveness of the fluids. Under certain operating conditions temperature cross over was observed in the heat exchanger.

In another recent work, characteristics of the flow in Chevron plate heat exchangers were examined through visualization tests of channels where Chevron angles are 28° and 65° . The correlations derived with the friction factor, f and Nusselt number, Nu for flow in channels of arbitrary geometry were used to evaluate thermal and hydraulic characteristics of the entrance. Then, experimental results were utilized to adjust the derived correlations. This paper is useful to

understand the mechanisms determining heat transfer and pressure drop in Chevron plate channels and the corresponding influence of the flow conditions and geometrical parameters. This study can be thought of as a continuation of Dović's thesis. In this study, the model focuses on the single cell, which is the smallest repeating unit of the channel composed of two crossing ducts with (close to) sinusoidal cross sections. In the experiments, injections of dye to the transparent wall or the central part of the single cell were used to visualize the flow in the channel. Solutions for the prediction of heat transfer and pressure drop in parallel heat exchanger channels have been provided to give results which are consistent with the experiments for a wide range of flow conditions and geometrical parameters. These solutions can be useful when no experimental data are available for a particular flow regime and geometry. This study can be improved with more experimental data for plates of various geometries.

Tsuzuki et al. proposed a new flow configuration, named S-shaped fin configuration to reduce the μ HEX pressure drop. A numerical study using a 3D-CFD code, FLUENT, was performed to find Nusselt number correlations for the μ HEX. A method to evaluate the heat transfer performance of the whole heat exchanger from the two correlations was proposed. The copper heat exchanger, whose dimensions are $1240 \times 68 \times 4.75 \text{ mm}^3$, comprises cold water channels and hot CO_2 channels. For both hot and cold sides, simulations were done to attain accurate empirical correlations for different temperatures. PROPATH, a database for thermo-physical properties of the fluids was used to for CO_2 . The results were in the neighborhood of 3% error when a comparison was made with other numerical studies. On the other hand, the difference between experimental results and the correlations was approximately 5%. Although the Reynolds number on the CO_2 side is sufficiently large to be regarded as turbulent flow, it was small for the water side. However, water flow showed rather more turbulent behavior than laminar, with Reynolds number less than 1500. The results indicate that the pressure drop of the S-shaped fin configuration was about one-seventh of that of

the conventional zigzag configuration while the heat transfer rate was almost identical.

One of the comprehensive studies in counter flow μ HEX area was done last year. In this work, numerical simulations were made to study the effect of the size and shape of channels; such as circular, square, rectangular, iso-triangular, and trapezoidal, in counter flow μ HEX. The results show that for the same volume of heat exchanger, increasing the number of channels leads to an increase in both effectiveness and pressure drop. Moreover, circular channels give the best overall performance (thermal and hydraulic) among various channel shapes. The second best overall performance is provided by square channels. New correlations are developed to predict the value of heat exchanger effectiveness and performance index as a function of the relative size of the channels with overall heat exchanger volume, Reynolds number, and thermal conductivity ratio.

Recently, an experimental analysis of two designed μ HEX, whose cross sectional areas are 100×100 and $200 \times 200 \mu\text{m}^2$, was performed to compare with the predictions of the classical viscous flow and heat transfer theory. The working fluid was deionized water. The minimum Reynolds number of each current was defined by the minimum flow rate that could steadily be controlled by the pump. The maximum Reynolds number was restricted by the maximum flow rate of the pump, which was 1 L/min, and occasionally the pressure drop, which cannot be larger than 4 bars, to avoid leaks. The results showed good agreement with the general theory and no special effect related to the small dimensions of the channels was observed. On the other hand, the author mentioned that the plate conduction thermal resistance is a major restriction for μ HEX performance. For the current thesis, the plate thickness and plate material are critical in the design of the μ HEX.

In another work, Schgulla et al. investigated a heat exchanger made of plastic with heat fluxes up to 500 W/cm^2 , a pressure drop of 0.16 MPa, and mass

flow of water 200 kg/h per passage. The use of plastic results in higher temperature resistance, higher stability, higher water throughputs and higher flow velocities. The specific fluid data of deionized water have been assumed to be constant in the temperature range between 10°C and 95°C.

Kang and Tseng theoretically modeled thermal and fluidic characteristics of a cross-flow μ HEX assuming that flows in rectangular channels, where fin height and width are 32 μm and 200 μm respectively, are incompressible, steady, and laminar. They compared the theoretical solutions with the experimental data from the available literature and validated the theoretical model. The interactive effect between the effectiveness and pressure drop in the μ HEX was analyzed. Besides, they showed that the heat transfer rate and the pressure drop at the same effectiveness value are significantly affected by the average temperature of the hot and cold side flow. The results were confirmed by Kang and Tseng as they indicated that different effectiveness values influence heat transfer and pressure drop considerably. The effect of the change of the μ HEX material from silicon to copper and dimensions were also investigated. A small volume of the heat exchanger (i.e. 9 x 9 x 10.2 mm) enables almost the same temperature distribution. In their study, the surface temperature on the wall of the heat exchanger was assumed as constant. Steady heat transfer rate and constant solid and fluid properties were used. Pressure drop, flow rates, inlet and outlet temperatures from both sides of the heat exchanger were measured in experiments. The temperatures difference between cold and hot fluids' inlets and outlets were measured to be 10°C under same effectiveness value ($\epsilon=0.333$). Kang and Tseng could achieve a heat transfer rate larger than 2700W for different average temperatures. Their study shows that under the same effectiveness value, a small rise in the temperatures of working fluids results in an increase of the heat transfer rate, but a decrease in pressure drop occurs. An increase in effectiveness causes a decrease if both the heat transfer rate and pressure drop. The experiments showed that a better heat transfer rate can be achieved by small effectiveness values. Kang and Tseng claimed that enlarging the dimensions of the heat exchanger has some

advantages and disadvantages regarding the pressure drop and the heat transfer rate; an optimization must be done according to design criteria. For example, by only doubling the size of the heat exchanger without changing fin parameters, the heat transfer rate increases from 2700 W to 22000 W; however, the pressure drop also increases about three-to-four times.

Vamadevan and Kraft used aluminum brazing to produce a microchannel tube heat exchanger. They investigated the effect of processing on the mechanical behavior of aluminum brazing on the microchannel tube heat exchanger. Commercially extruded and processed AA3102 microchannel tube was exposed to a brazing thermal cycle. A special apparatus was developed to provide pressure test capabilities up to 69 MPa (10,000 psi), and simultaneous sample heating up to 180°C for microchannel tube samples. This paper is useful to understand the behavior of microchannel after brazing process.

Wen et al. used CFD simulation, FLUENT, and PIV (Particle Image Velocymeter) to determine the turbulent flow structure inside the entrance of a plate fin heat exchanger. PIV is an instantaneous whole-field measurement technique, which uses a pulsed light-sheet to illuminate a gas flow seeded with tracer particles. By means of PIV, a series of velocity vectors and streamline graphs of different cross sections are obtained. The turbulence flow was calculated by the Semi-implicit SIMPLER Algorithm method in the velocity and pressure conjugated problem, and a second order upwind differential scheme was applied for the approximation of the convective terms. The computation and experiment were performed under the similar inlet Reynolds number ($Re = 6.0 \times 10^4$). CFD results and PIV data were in good agreement with each other. The authors conclude that PIV and CFD are well suitable to analyze complex flow patterns.

A few years ago, Foli et al. introduced multi-objective genetic algorithms for determining the optimal geometric parameters of the microchannel in μ HEX to maximize the heat transfer rate under specified design constraints. CFD

analysis with an analytical method of calculating the optimal geometric parameters was also performed. This paper is important and a good work, because there is limited published literature on attempts at designing μ HEX for optimal performance. This work is different from the other studies in that a commercial CFD analysis program, CFD-ACE+ has been used.

Nika et al. introduced new techniques to analyze heat exchangers. The scope of their work was thermoacoustic phenomena in multi-channel heat exchangers, without phase change of the fluid. In this study, microchannel were made of silicon by means of LIGA (Lithography Galvano Abformung) technique. The authors listed three factors, which are thermal characteristic time, aerodynamic matrix of transfer, and thermal efficiency, to analyze the aerodynamic and thermal performance of a μ HEX. This work concerns only situations where the displacement of the fluid is considerably smaller than the length of the heat exchanger itself, and abrupt changes of the wall temperature or of the section are also prohibited.

Kanlayasairi and Paul worked on a fabrication procedure for NiAl microchannel arrays [32]. For leakage tests, they made a similar work as the current work. This paper introduced a microlamination procedure for producing high-aspect-ratio NiAl microchannel arrays. Several 28:1 aspect ratio NiAl microchannel arrays were produced. Metallography was conducted to evaluate the geometry of the microchannel. Reactive diffusion bonding was introduced as a joining technique for NiAl lamina. Laser micromachining was applied to cut the NiAl lamina without thermal cracking.

Jiang et al. performed an experimental comparison of μ HEX with microchannel and porous media. The effect of the dimensions on heat transfer was analyzed numerically. It was emphasized that the heat transfer performance of the μ HEX using porous media is better than that of the μ HEX using microchannel, but the pressure drop of the former is much larger.

As mentioned before there is a substantial research on microchannel and heat sinks. Recently, Alpsan performed a research on microchannel heat sinks for phased array radar cooling application. In this research, experimental measurements and numerical simulations were performed on copper and aluminum microchannel heat sinks of 300, 420, 500, and 900 μm channel widths. Alpsan designed the heat sinks specifically for use with T/R (transmit/receive) module cooling applications of military phased array radars. An analytical calculation was also performed to aid in the design methodology. Alpsan used a chip carrier mounted with attenuators to simulate the localized head load of actual transmit/receive modules. Distilled water was used as the coolant with flow rates ranging from 0.50 lpm (liters per minute) to 1.00 lpm. Local heat fluxes as high as 100 W/cm^2 were tested. Temperature measurements were taken by thermistors on the heat load surface and by J-type thermocouples in the water and air regions. Pressure measurements were taken by pressure transducers at the heat sink inlet and outlet regions. A digital output flow meter was used to record the coolant flow rate. In his study, experimental results showed that copper specimens were significantly superior to aluminum specimens in terms of cooling performance, as expected, due to their difference in thermal conductivity. The thermally best performing specimen, the 300 μm copper specimen, yielded a maximum temperature rise of 26.1°C between the heat load and coolant inlet, at a coolant flow rate of 1.00 lpm and local heat flux of 100 W/cm^2 , leading to a thermal resistance of 0.63°C/W . The pressure drop measured across the heat sink under these conditions was 0.030 bars. The experimental results regarding thermal performance were observed to be consistent when compared to similar studies in the literature. Results for pressure drop, however, showed significant departure. This was attributed to the geometrical differences in the heat sinks between studies compared. Alpsan also carried out numerical simulations using the commercial Computational Fluid Dynamics (CFD) software FLUENT[®]. Effects of thermal interface layers and heat spreading due to the localized heat load were investigated. Simulation results for temperature were seen to agree fairly well with experimental data as long as thermal interface layers were accounted for. The

simple analytical calculation for temperature, based on the classical fin approach, deviated greatly from experimental results due to the thermal interface and heat spreading effects not being included in the calculation. The analytical calculation for pressure drop, based on conventional theory for developing flow, coincided perfectly with the numerical results. This study showed that the T/R modules of military phased array radars, dissipating as high as 100 W/cm^2 locally, could be cooled within the limits of the harsh environmental conditions required of military applications with moderate pressure drops.

Philips investigated fluid flow and heat transfer in microchannel experimentally and numerically. Fluid flow and heat transfer experiments were conducted on a copper μHEX . An experimental method of imposing a constant surface temperature to the μHEX was used. In this study, the friction factor results from the experiments agreed fairly well with theoretical correlations and moreover the experimental Nusselt number results agreed with theory very well in the transition/turbulent regime, but the results show a higher Nusselt number in the laminar regime than predicted by theoretical correlations. Philips created a CFD model to simulate the fluid in the inlet plenum and the microchannel. The results from these simulations showed good agreement with the experimental data in the transition/turbulent regime as well as with theoretical correlations for laminar and turbulent flow.

Literature shows that the microchannel and microchannel heat sinks were studied extensively, but there is limited research related to the performance of two fluid microchannel heat exchangers and there are not much comprehensive investigations to study the effect of channels shape on the performance of two fluids cross flow μHEX . However, there has been an increase on this subject in the past few years.

CHAPTER 3

THEORY OF HEAT EXCHANGERS

In this chapter, basic heat transfer equations will be outlined for the thermal analysis of a μ HEX. Performance calculations of the heat exchanger (rating problem) will be carried out. First, heat transfer from the hot fluid to the cold fluid will be determined. Then effective mean temperature difference of the fluids inlet and outlet temperatures will be investigated to determine the heat transfer. The overall heat transfer coefficients will be introduced in this analysis. Next, fin efficiency and overall surface efficiency will be explained. Heat transfer effectiveness, heat capacity rate ratios and number of transfer unit will be determined. To determine the convective heat transfer coefficient some dimensionless numbers will be introduced. Finally, geometrical properties will be analyzed to find the hydraulic diameter of both sides.

3.1 Heat Transfer Analysis

Under steady state conditions with negligible potential and kinetic energy changes, if the fluids do not undergo a phase change and have constant specific heats, c_p and there is negligible heat transfer between the exchanger and its surroundings, for hot and cold fluids, heat transfer rate may be expressed as below

$$Q = (\dot{m} \cdot c_p)_h \cdot (T_{h1} - T_{h2}) \quad (1)$$

and

$$Q = (\dot{m} \cdot c_p)_c \cdot (T_{c2} - T_{c1}) \quad (2)$$

where \dot{m} is the rate of mass flow? The subscripts h and c refer to the hot and cold fluids, respectively and the numbers 1 and 2 designate the fluid inlet and outlet conditions, respectively. As cold fluid enthalpy increases and hot fluid enthalpy decreases, heat will be transferred from the hot fluid to the cold fluid.

The temperature difference between the hot and cold fluids varies with position in the heat exchanger. Therefore, in the heat transfer analysis of heat exchangers, it is convenient to establish an appropriate mean value of the temperature difference between the hot and cold fluids such that the total heat transfer rate Q between the fluids can be determined from the following equation:

$$Q = U \cdot A \cdot \Delta T_{lm} \quad (3)$$

Here, A is the total hot side or cold side heat transfer area and U is the overall heat transfer coefficient based on that area. ΔT_{lm} is the effective mean temperature difference and is a complex function of T_{h1} , T_{h2} , T_{c1} , T_{c2} . ΔT_{lm} can be determined analytically in terms of the following quantities:

$$\Delta T_{lm,cf} = \frac{(T_{h2}-T_{c1})-(T_{h1}-T_{c2})}{\ln \left[\frac{T_{h2}-T_{c1}}{T_{h1}-T_{c2}} \right]} \quad (4)$$

$$P = \frac{T_{c2}-T_{c1}}{T_{h1}-T_{c1}} = \frac{\Delta T_c}{\Delta T_{max}} \quad (5)$$

$$R = \frac{C_c}{C_h} = \frac{T_{h1}-T_{h2}}{T_{c2}-T_{c1}} = \frac{\Delta T_h}{\Delta T_c} \quad (6)$$

Here, $\Delta T_{lm,cf}$ is the log mean temperature difference (LMTD) for a counterflow arrangement with the same fluid inlet and outlet temperatures. P is a measure of the ratio of the heat actually transferred to the heat which would be transferred if the same cold fluid temperature was raised to the hot fluid temperature; therefore, P is the temperature effectiveness of the heat exchanger on the cold fluid side. R is the ratio of the heat capacity rate ($\dot{m}c_p$) of the cold fluid to that of the hot fluid and it is called the heat capacity rate ratio.

ΔT_{lm} may also be used for multipass and crossflow heat exchangers by multiplying it with a correction factor F

$$Q = U \cdot A \cdot \Delta T_{lm} = U \cdot A \cdot F \cdot \Delta T_{lm,cf} \quad (7)$$

F is no dimensional and depends on the temperature effectiveness P, the heat capacity ratio R and the flow arrangement

$$F = \phi(P, R, \text{flow arrangement}) \quad (8)$$

The correction factor F is less than unity for crossflow and multi-pass arrangements. The correction factor for crossflow and multi-pass arrangement is available in graphical form in Ref .For a crossflow heat exchanger with both fluids unmixed Fig. 3.1 is used.

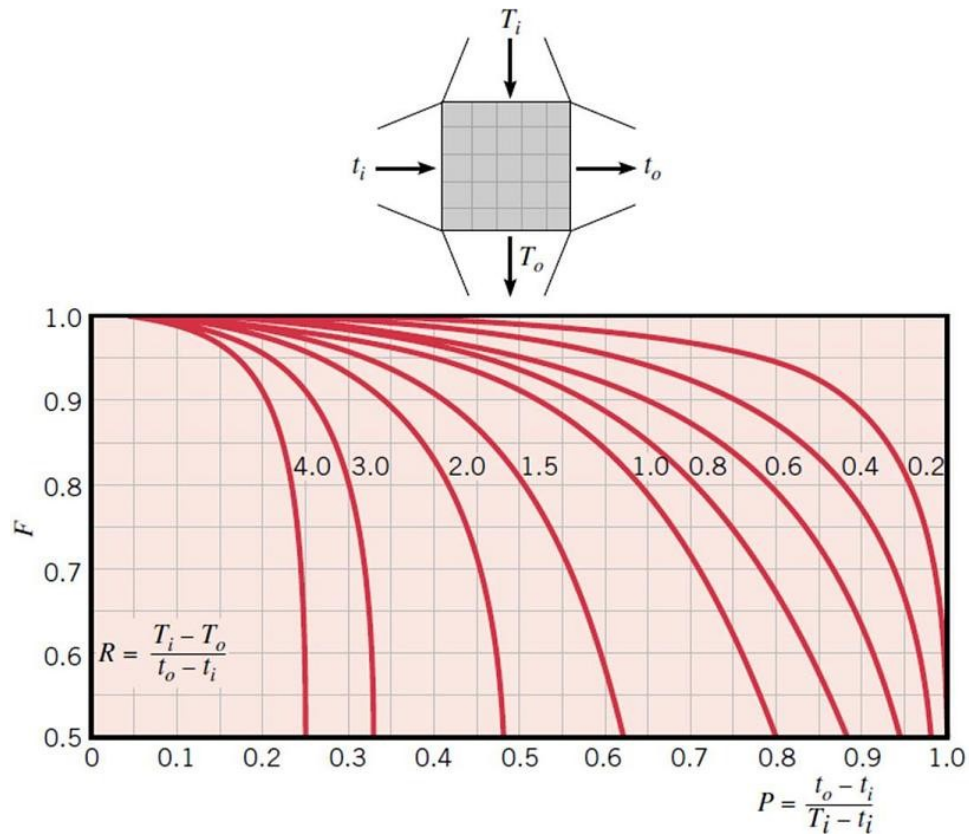


Figure 3.1: LMTD correction factor F for a single pass crossflow heat exchanger with both fluids unmixed

3.2 Overall Thermal Coefficient, UA

At steady state, heat is transferred from the hot fluid to the cold fluid with the following processes: convection to the hot fluid wall, conduction through the wall and subsequent convection from the wall to the cold fluid. In many heat exchangers, a fouling film is formed as a result of accumulation of scale or rust formation, deposits from fluid, chemical reaction products between the fluid and the wall material or biological growth. Fouling results in an additional insulating layer to the heat transfer surface. As a result, the total thermal resistance includes the thermal convection resistances of both sides, the wall resistance and fouling resistances of both sides.

$$R_t = R_h + R_{f,h} + R_w + R_{f,c} + R_c \quad (9)$$

where

$$R_h = \frac{1}{(\eta_{0,h} \cdot h \cdot A)_h} \quad (10)$$

$$R_{f,h} = \frac{R_{fh}}{\eta_{0,h} \cdot A_h} \quad (11)$$

$$R_w = \frac{\delta_w}{k_w \cdot A_w} \quad (12)$$

$$R_{f,c} = \frac{R_{fc}}{\eta_{0,c} \cdot A_c} \quad (13)$$

$$R_c = \frac{1}{(\eta_{0,c} \cdot h \cdot A)_c} \quad (14)$$

In Eqs. (15-20), R_h and R_c represent the convection resistances of hot and cold fluids with finned surfaces, respectively. The separating wall resistance is shown as R_w . R_{fh} and R_{fc} represent the fouling resistances of hot and cold sides respectively. It is extremely difficult to predict a specific fouling behavior for most cases since a large number of variables can materially alter the type fouling and its rate of formation. Sources of fouling resistance in the literature are rather limited. The most referenced source of fouling factors is in the standards of the Tubular Exchanger Manufacturers Association, available in Ref.

The total thermal resistance is also expressed as the inverse of overall thermal coefficient.

$$R_t = \frac{1}{U \cdot A} \quad (15)$$

The overall thermal coefficient UA may be defined optionally in terms of the surface area of the hot surface or the cold surface or the wall conduction wall areas.

$$UA = U_h \cdot A_h = U_c \cdot A_c = U_w \cdot A_w \quad (16)$$

$$UA = \left(\frac{1}{(\eta_{0,h} \cdot h \cdot A)_h} + \frac{R_{fh}}{\eta_{0,h} \cdot A_h} + \frac{\delta_w}{k_w \cdot A_w} + \frac{R_{fc}}{\eta_{0,c} \cdot A_c} + \frac{1}{(\eta_{0,c} \cdot h \cdot A)_c} \right)^{-1} \quad (17)$$

3.3 Fin Efficiency

The η in thermal resistances represents fin efficiency. In most two-fluid plate fin heat exchangers, fins are used to increase the surface area and consequently, to increase the total rate of heat transfer. Assuming there is no heat transfer through the center of the fin and it is treated as adiabatic, the fin efficiency of a plain fin is:

$$\eta_f = \frac{\tanh(m \cdot l_1)}{m \cdot l_1} \quad (18)$$

where

$$m = \left[\frac{2 \cdot h}{k_f \cdot \delta} \left(1 + \frac{\delta}{L_f} \right) \right]^{1/2} \quad (19)$$

$$l_1 = \frac{b}{2} - \delta \quad (20)$$

where b is the fin height (the distance between two plates in the heat exchanger), δ is the fin thickness, l_1 is the adiabatic fin height, L_f is the fin length and k_f is thermal conductivity of fin and h is the convection heat transfer coefficient.

The overall surface efficiency is expressed as:

$$\eta_0 = \left[1 - (1 - \eta_f) \cdot \frac{A_f}{A} \right] \quad (21)$$

3.4 Heat Exchanger Effectiveness and NTU

Heat capacity rate ratio, C^* is the ratio of the smaller to the larger heat capacity rate of hot and cold fluids.

$$C^* = \frac{C_{min}}{C_{max}} \quad (22)$$

where

$$C_{min} = \min(C_c, C_h) \quad (23)$$

$$C_{max} = \max(C_c, C_h) \quad (24)$$

$$C_c = (\dot{m} \cdot c_p)_c \quad (25)$$

$$C_h = (\dot{m} \cdot c_p)_h \quad (26)$$

The fluid that might undergo the maximum temperature difference is the fluid with the minimum heat capacity rate. The maximum heat transfer is expressed as:

$$Q_{max} = (\dot{m} \cdot c_p)_c \cdot (T_{h1} - T_{c1}) \quad \text{if } C_c < C_h \quad (27)$$

$$Q_{max} = (\dot{m} \cdot c_p)_h \cdot (T_{h1} - T_{c1}) \quad \text{if } C_h < C_c \quad (28)$$

Effectiveness is a measure of the thermal performance of a heat exchanger and can be defined as the ratio of the actual heat transfer rate to the thermodynamically limited maximum possible heat transfer rate.

$$\varepsilon = \frac{Q}{Q_{max}} = \frac{C_h \cdot (T_{h1} - T_{h2})}{C_{min} \cdot (T_{h1} - T_{c1})} = \frac{C_c \cdot (T_{c2} - T_{c1})}{C_{min} \cdot (T_{h1} - T_{c1})} \quad (29)$$

The number of transfer units, NTU , designates the no dimensional heat transfer size of the heat exchanger and is defined as a ratio of the overall thermal conductance to the minimum heat capacity rate:

$$NTU = \frac{U \cdot A}{C_{min}} \quad (30)$$

Effectiveness can be expressed as function of NTU *and*. The derivation of $\varepsilon - NTU$ expressions is complicated. For a cross-flow and unmixed flow arrangement, an equation is available.

$$\begin{aligned} \varepsilon = 1 - e^{-(1+C^*) \cdot NTU} \cdot [I_0(2 \cdot NTU \cdot \sqrt{C^*}) \\ + \sqrt{C^*} \cdot I_1(2 \cdot NTU \cdot \sqrt{C^*}) \\ - \frac{1-C^*}{C^*} \cdot \sum_{n=2}^{\infty} C^{*\frac{n}{2}} \cdot I_n(2 \cdot NTU \cdot \sqrt{C^*})] \end{aligned} \quad (31)$$

Here, I_0, I_1, I_n are the modified Bessel functions. Moreover, ε vs. NTU is available in Ref.

3.5 Pressure Drop

The amount of pressure drop of both fluids is an important part of performance analysis. It is difficult to predict the pressure drop in a non-standard heat exchanger. Therefore, in this work, pressure drop will be determined using the measured difference in pressure at the inlet and outlet of the heat exchanger for both fluids.

$$\Delta p_h = p_{h1} - p_{h2} \quad (32)$$

$$\Delta p_c = p_{c1} - p_{c2} \quad (33)$$

where p_{h1}, p_{c1} are inlet pressure of hot and cold fluids respectively and outlet pressures are, p_{h2} and p_{c2} .

3.6 Heat Transfer Coefficient

For the determination of convection heat transfer coefficient h , some dimensionless numbers will be introduced.

The Reynolds number, Re , is interpreted as a flow characteristic proportional to the ratio of flow momentum rate to viscous force for a specified geometry. Re is also called as flow modulus and defined for internal flow as

$$Re = \frac{G \cdot D_h}{\mu} \quad (34)$$

and

$$G = \frac{\dot{m}}{A_0} = \rho \cdot u_m \quad (35)$$

where A_0 is the cross sectional area, ρ is the density, μ is the viscosity of fluid and u_m is the mean fluid velocity. For internal flows, if $Re < 2300$ then the flow is laminar. D_h is defined for noncircular ducts and is expressed as:

$$D_h = 4 \cdot \frac{A_c}{p} = \frac{4 \cdot (\text{net free flow area})}{\text{wetted perimeter}} \quad (36)$$

The Nusselt number, Nu , is one of the dimensionless representations of the heat transfer coefficient. Nu is a ratio of the convective conductance to pure molecular thermal conductance over the hydraulic diameter. It is defined as:

$$Nu = \frac{h \cdot D_h}{k} \quad (37)$$

Here, k is the thermal conductivity of the fluid.

The Stanton number, St , is the ratio of convection heat transfer to the enthalpy rate change of the fluid reaching the wall temperature. St does not depend on any geometrical characteristic dimension. It is defined as:

$$St = \frac{h}{G \cdot c_p} \quad (38)$$

The Brandt number, PR , is the fluid property modulus representing the ratio of momentum diffusivity to thermal diffusivity of the fluid. PR is expressed as:

$$Pr = \frac{\nu}{\alpha} = \frac{\mu \cdot c_p}{k} \quad (39)$$

The Colburn factor, j , is the modified Stanton number to take into account the moderate variations in the fluid Prandtl number. It is defined as:

$$j = St \cdot Pr^{2/3} = \frac{Nu \cdot Pr^{-1/3}}{Re} \quad (40)$$

For a rectangular channel, Nu depends on the channel aspect ratio $\alpha_c = \frac{a}{b}$ (where a is the short length of a rectangular profile and b is the long length of rectangular profile) and the wall boundary conditions. For liquid flow in rectangular microchannel, fully developed laminar flow and taking into account temperature variations of liquid, Nu can be expressed as below:

$$Nu = [8.235 \cdot (1 - 1.883 \cdot \alpha_c + 3.767 \cdot \alpha_c^2 - 5.814 \cdot \alpha_c^3 + 5.361 \cdot \alpha_c^4 - 2 \cdot \alpha_c^5)] \cdot \left(\frac{\mu_b}{\mu_w}\right)^{-0.14} \quad (41)$$

The subscripts b and w designate properties evaluated at the bulk mean temperature and wall temperature respectively.

3.7 Geometrical Properties

The determination of geometrical characteristics for finned cross flow heat exchangers is somewhat complicated due to the presence of plain fins. The plain fin used can be assumed as rectangular. However, in reality the rectangular fin geometry has rounded corners instead of the sharp corners as shown in Fig. 3.2. The primary surface area and secondary (fin) surface area associated with a rectangular fin are also shown in Figs. 3.2 and 3.3. These sketches represent a good approximation due to the braze fillet and radius.

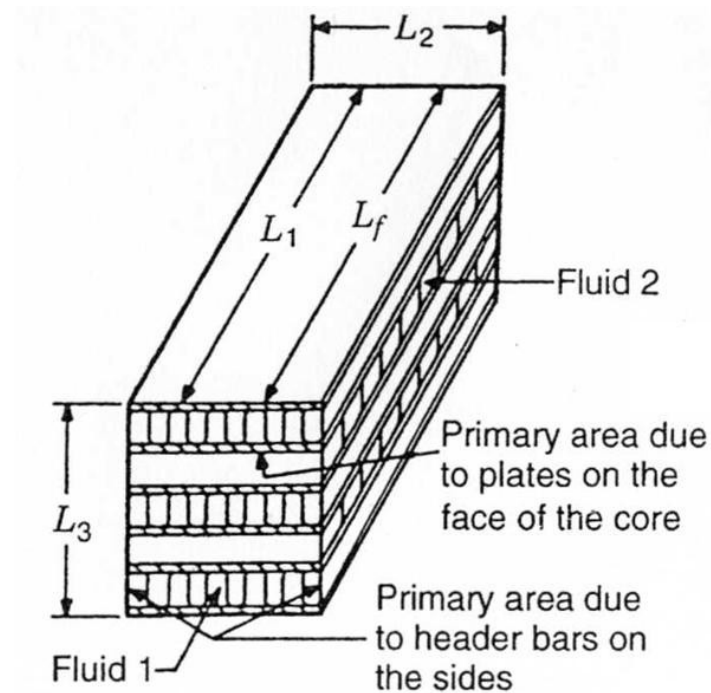


Figure 3.2: Cross flow plain fin heat exchanger

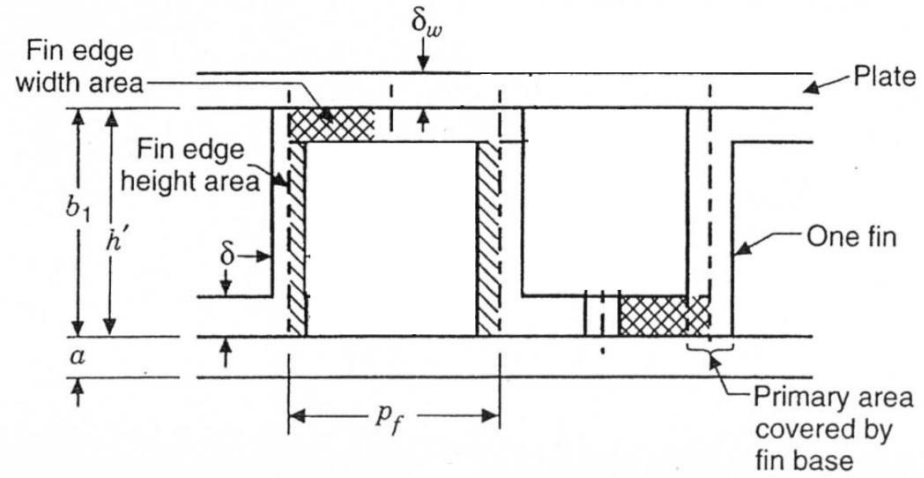


Figure 3.3: Idealized plain rectangular fin [1]

The total heat transfer area A for fluid 1 consists of primary, A_p and secondary (fin), A_f surface area swept by fluid 1, and is identical for fluid 2 due to the symmetrical conditions of the heat exchanger. The following four components are needed for calculating the primary surface area:

- (1) plate area,
- (2) fin base area that covers the plate,
- (3) header bar area on the sides for fluid 1 near the ends of fins in the L_2 direction
- (4) header bars and plates exposed area of the blocked fluid 2 passage at fluid 1 core inlet and outlet faces.

The secondary (fin) area consists of

- (1) fin height area,
- (2) fin edge height area
- (3) fin edge width area.

The primary surface area is then the sum of components 1, 3 and 4 minus component 2. These four components of the primary surface area are now derived as:

$$\text{total plate area} = 2 \cdot L_1 \cdot L_2 \cdot N_p \quad (42)$$

where N_p is the total number of fluid 1 passages in the L_3 direction.

$$\text{fin base area covering plates} = 2 \cdot \delta \cdot L_f \cdot n_f \quad (43)$$

$$= 2 \cdot \delta \cdot L_f \cdot N_f \cdot L_2 \cdot N_p \quad (44)$$

where L_f is the fin flow length, $n_f = N_f L_2 N_p$ is the total number of fins in the core and N_f is the number of fins per unit length in the L_2 direction. The fin flow length is slightly shorter than the core flow length L_1 in an actual core.

$$\text{area of header bars on the side for fluid 1} = 2 \cdot b_1 \cdot L_1 \cdot N_p \quad (45)$$

$$\text{area of header bars and plates of fluid 2 at fluid 1 core inlet and outlet faces} = 2 \cdot (b_2 + 2 \cdot \delta_w) \cdot (N_p + 1) \cdot L_2 \quad (46)$$

The total primary surface area on the fluid 1 side is then

$$A_{p,1} = 2 \cdot L_1 \cdot L_2 \cdot N_p - 2 \cdot \delta \cdot L_f \cdot N_f \cdot L_2 \cdot N_p + 2 \cdot b_1 \cdot L_1 \cdot N_p + 2 \cdot (b_2 + 2 \cdot \delta_w) \cdot (N_p + 1) \cdot L_2 \quad (47)$$

The three components of the secondary (fin) area are:

$$\text{fin height area} = 2 \cdot (b_1 - \delta) \cdot L_f \cdot n_f \quad (48)$$

$$\text{fin edge height area} = 2 \cdot (b_1 - \delta) \cdot \delta \cdot n_f \quad (49)$$

$$\text{fin edge width area} = 2 \cdot p_f \cdot \delta \cdot n_f \quad (50)$$

The total secondary area on fluid 1 side is:

$$A_{f,1} = 2 \cdot (b_1 - \delta) \cdot L_f \cdot n_f + 2 \cdot (b_1 - \delta) \cdot \delta \cdot n_f + 2 \cdot p_f \cdot \delta \cdot n_f \quad (51)$$

Finally, the total surface area on fluid 1 side is:

$$A_1 = A_{p,1} + A_{f,1} \quad (52)$$

The free flow area on fluid 1 side is given by the frontal area on fluid 1 side minus the area blocked by the fins at the entrance of the core on that side:

$$A_{0,1} = b_1 \cdot L_2 \cdot N_p - [(b_1 - \delta) + p_f] \cdot \delta \cdot n_f \quad (53)$$

Moreover, the hydraulic diameter can be expressed using surface parameters as follows:

$$D_{h,1} = \frac{4 \cdot A_{0,1} \cdot L_1}{A_1} \quad (54)$$

CHAPTER 4

SAMPLE CALCULATIONS

4.1 Geometrical Parameters

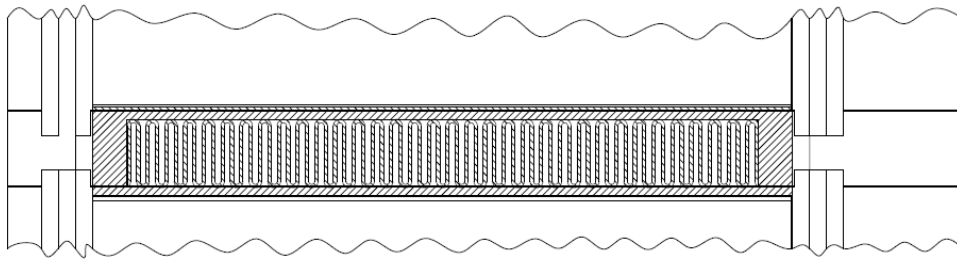


Figure A.1: Section view of the heat exchanger

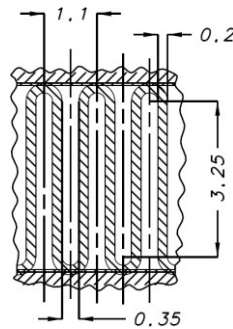


Figure A.2: Detailed section view of water side of the heat exchanger

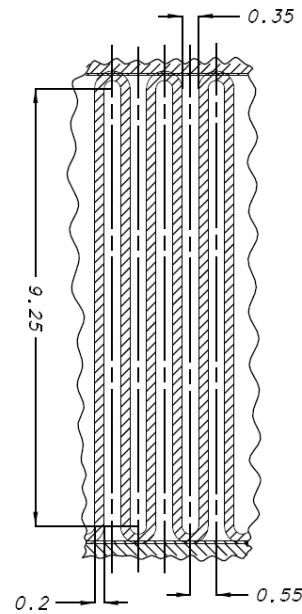


Figure A.3: Detailed section view of air side of the heat exchanger

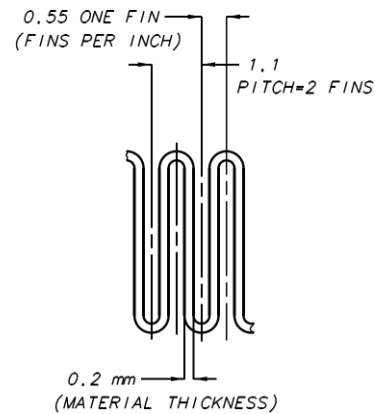


Figure A.4: Detailed view of plain fin of both sides of the heat exchanger

All detailed drawings of the heat exchanger are given in Appendix C. From drawings in Appendix C and Fig. A.2, A.3 and A.4, geometrical parameters for the heat exchanger may be determined.

Fin thickness for both air and water side

$$\delta_c = \delta_h = 0.2 \text{ mm}$$

Fin height for airside

$$b_c = b_2 = 10 \text{ mm}$$

Fin height for waterside	$b_h = b_1 = 4 \text{ mm}$
One fin width for both sides	$p_f = 0.55 \text{ mm}$
Fin flow length for airside	$L_{f,c} = 40 \text{ mm}$
Fin flow length for waterside	$L_{f,h} = 80 \text{ mm}$
Number of fins per unit length for air side	$N_{f,c} = 46 \text{ fin/inch}$
Number of fins per unit length for water side	$N_{f,h} = 46 \text{ fin/inch}$
Total number of water passage	$N_{p,h} = 6$
Total number of air passage	$N_{p,c} = N_{p,h} + 1$ $N_{p,c} = 7$
Wall thickness between air and water passage	$\delta_w = 1 \text{ mm}$
Length of heat exchanger in flow direction of water	$L_1 = 85 \text{ mm}$
Length of heat exchanger in flow direction of air for water side	$L_{2,h} = 37 \text{ mm}$
Length of heat exchanger in flow direction of water for air side	$L_{2,c} = 41 \text{ mm}$
Height of heat exchanger	$L_3 = 110 \text{ mm}$

From Fig. A.2 and A.3 it can be assumed that flow passages of both side rectangular channel. After assuming rectangular channel of flow passages first aspect ratio of both sides will be calculated.

For water sides From Fig. A.2, the dimensions of rectangular will be:

$$a_h = 0.35 \text{ mm}$$

$$b_h = 3.55 + 0.2 = 3.75 \text{ mm}$$

Then, aspect ratio for water channel:

$$\alpha_{c,h} = \frac{a_h}{b_h} = \frac{(0.35 \text{ mm})}{(3.75 \text{ mm})} = 0.0933$$

For air side From Fig. A.3, the dimensions of rectangular will be:

$$a_c = 0.35 \text{ mm}$$

$$b_c = 9.55 + 0.2 = 9.75 \text{ mm}$$

Then, aspect ratio for air channel:

$$\alpha_{c,c} = \frac{a_c}{b_c} = \frac{(0.35 \text{ mm})}{(9.75 \text{ mm})} = 0.0359$$

4.2 Surface Geometrical Properties

To find hydraulic diameter of both sides, primary and secondary surface areas will be calculated.

Water Side

Total plate area

$$= 2 \cdot L_1 \cdot L_2 \cdot N_p = 2 \cdot (85 \text{ mm}) \cdot (37 \text{ mm}) \cdot (6) = 37740 \text{ mm}^2$$

Fin base area covering plates

$$\begin{aligned} &= 2 \cdot \delta \cdot L_f \cdot n_f = 2 \cdot \delta \cdot L_f \cdot N_f \cdot L_2 \cdot N_p \\ &= 2 \cdot (0.2 \text{ mm}) \cdot (80 \text{ mm}) \cdot \left(46 \frac{\text{fin}}{25.4 \text{ mm}}\right) \cdot (37 \text{ mm}) \cdot (6) = 12865.512 \text{ mm}^2 \end{aligned}$$

Area of header bars on the side for water

$$= 2 \cdot b_1 \cdot L_1 \cdot N_p = 2 \cdot (4 \text{ mm}) \cdot (85 \text{ mm}) \cdot (6) = 4080 \text{ mm}^2$$

Area of header bars and plates of air at water core inlet and outlet faces

$$\begin{aligned}
&= 2 \cdot (b_2 + 2 \cdot \delta_w) (N_p + 1) L_2 \\
&= 2 \cdot (10 \text{ mm} + 2 \cdot (1 \text{ mm})) \cdot (6 + 1) \cdot (37 \text{ mm}) = 6216 \text{ mm}^2
\end{aligned}$$

The total primary surface area on the water side is then

$$\begin{aligned}
A_{p,1} &= 2 \cdot L_1 \cdot L_2 \cdot N_p - 2 \cdot \delta \cdot L_f \cdot N_f \cdot L_2 \cdot N_p + 2 \cdot b_1 \cdot L_1 \cdot N_p \\
&\quad + 2 \cdot (b_2 + 2 \cdot \delta_w) (N_p + 1) L_2 \\
&= (37740 \text{ mm}^2) - (12865.512 \text{ mm}^2) + (4080 \text{ mm}^2) + (6216 \text{ mm}^2) = 35170.488 \text{ mm}^2
\end{aligned}$$

The three components of the secondary (fin) area are:

Fin height area

$$\begin{aligned}
&= 2 \cdot (b_1 - \delta) \cdot L_f \cdot n_f \\
&= 2 \cdot (4 - 0.2) \cdot (80 \text{ mm}) \cdot \left(46 \frac{\text{fin}}{25.4 \text{ mm}}\right) \cdot (37 \text{ mm}) \cdot (6) = 244444.724 \text{ mm}^2
\end{aligned}$$

Fin edge height area

$$\begin{aligned}
&= 2 \cdot (b_1 - \delta) \cdot \delta \cdot n_f \\
&= 2 \cdot (4 - 0.2) \cdot (0.2) \cdot \left(46 \frac{\text{fin}}{25.4 \text{ mm}}\right) \cdot (37 \text{ mm}) \cdot (6) = 611.112 \text{ mm}^2
\end{aligned}$$

Fin edge width area

$$\begin{aligned}
&= 2 \cdot p_f \cdot \delta \cdot n_f \\
&= 2 \cdot (0.55 \text{ mm}) \cdot (0.2) \cdot \left(46 \frac{\text{fin}}{25.4 \text{ mm}}\right) \cdot (37 \text{ mm}) \cdot (6) = 88.450 \text{ mm}^2
\end{aligned}$$

The total secondary area on water side is:

$$\begin{aligned}
A_{f,1} &= 2 \cdot (b_1 - \delta) \cdot L_f \cdot n_f + 2 \cdot (b_1 - \delta) \cdot \delta \cdot n_f + 2 \cdot p_f \cdot \delta \cdot n_f \\
&= (244444.724 \text{ mm}^2) + (611.112 \text{ mm}^2) + (88.450 \text{ mm}^2) = 245144.287 \text{ mm}^2
\end{aligned}$$

The total surface area on water side is:

$$\begin{aligned} A_1 &= A_{p,1} + A_{f,1} \\ &= (35170.488 \text{ mm}^2) + (245144.287) \text{ mm}^2 = 280314.775 \text{ mm}^2 \end{aligned}$$

The free flow area on water side is given by the frontal area on water side minus the area blocked by the fins at the entrance of the core on that side:

$$\begin{aligned} A_{0,1} &= b_1 \cdot L_2 \cdot N_p - [(b_1 - \delta) + p_f] \cdot \delta \cdot n_f \\ &= (4 \text{ mm}) \cdot (37 \text{ mm}) \cdot (6) - [(4 \text{ mm} - 0.2 \text{ mm}) + (0.55 \text{ mm})] \\ &\quad \cdot (0.2 \text{ mm}) \cdot \left(46 \frac{\text{fin}}{25.4 \text{ mm}}\right) \cdot (37 \text{ mm}) \cdot (6) = 538.219 \text{ mm}^2 \end{aligned}$$

Air Side

Total plate area

$$\begin{aligned} &= 2 \cdot L_2 \cdot L_1 \cdot (N_p + 1) \\ &= 2 \cdot (41 \text{ mm}) \cdot (85 \text{ mm}) \cdot (7) = 48790 \text{ mm}^2 \end{aligned}$$

Fin base area covering plates

$$\begin{aligned} &= 2 \cdot \delta \cdot L_f \cdot n_f = 2 \cdot \delta \cdot L_f \cdot N_f \cdot L_1 \cdot (N_p + 1) \\ &= 2 \cdot (0.2 \text{ mm}) \cdot (40 \text{ mm}) \cdot \left(46 \frac{\text{fin}}{25.4 \text{ mm}}\right) \cdot (85 \text{ mm}) \cdot (7) = 17240.945 \text{ mm}^2 \end{aligned}$$

Area of header bars on the side for air

$$= 2 \cdot b_1 \cdot L_1 \cdot N_p$$

$$= 2 \cdot (10 \text{ mm}) \cdot (41 \text{ mm}) \cdot (7) = 5740 \text{ mm}^2$$

Area of header bars and plates of water at air core inlet and outlet faces

$$\begin{aligned} &= 2 \cdot (b_1 + 2 \cdot \delta_w) N_p L_1 \\ &= 2 \cdot (4 \text{ mm} + 2 \cdot (1 \text{ mm})) \cdot (6) \cdot (85 \text{ mm}) = 6120 \text{ mm}^2 \end{aligned}$$

The total primary surface area on the air side is then

$$\begin{aligned} A_{p,2} &= 2 \cdot L_2 \cdot L_1 \cdot (N_p + 1) - 2 \cdot \delta \cdot L_f \cdot N_f \cdot L_1 \cdot (N_p + 1) \\ &\quad + 2 \cdot b_2 \cdot L_2 \cdot (N_p + 1) + 2 \cdot (b_1 + 2 \cdot \delta_w) N_p L_1 \\ &= (48790 \text{ mm}^2) - (17240.945 \text{ mm}^2) + (5740 \text{ mm}^2) + (6120 \text{ mm}^2) = 43409.055 \text{ mm}^2 \end{aligned}$$

The three components of the secondary (fin) area are:

Fin height area

$$\begin{aligned} &= 2 \cdot (b_2 - \delta) \cdot L_f \cdot n_f \\ &= 2 \cdot (10 - 0.2) \cdot (40 \text{ mm}) \cdot \left(46 \frac{\text{fin}}{25.4 \text{ mm}}\right) \cdot (85 \text{ mm}) \cdot (7) = 844806.299 \text{ mm}^2 \end{aligned}$$

Fin edge height area

$$\begin{aligned} &= 2 \cdot (b_2 - \delta) \cdot \delta \cdot n_f \\ &= 2 \cdot (10 - 0.2) \cdot (0.2) \cdot \left(46 \frac{\text{fin}}{25.4 \text{ mm}}\right) \cdot (85 \text{ mm}) \cdot (7) = 4224.031 \text{ mm}^2 \end{aligned}$$

Fin edge width area

$$\begin{aligned} &= 2 \cdot p_f \cdot \delta \cdot n_f \\ &= 2 \cdot (0.55) \cdot (0.2) \cdot \left(46 \frac{\text{fin}}{25.4 \text{ mm}}\right) \cdot (85 \text{ mm}) \cdot (7) = 237.063 \text{ mm}^2 \end{aligned}$$

The total secondary area on air side is:

$$A_{f,2} = 2 \cdot (b_2 - \delta) \cdot L_f \cdot n_f + 2 \cdot (b_2 - \delta) \cdot \delta \cdot n_f + 2 \cdot p_f \cdot \delta \cdot n_f$$

$$= (844806.299 \text{ mm}^2) + (4224.031 \text{ mm}^2) + (237.063 \text{ mm}^2) = 849267.961 \text{ mm}^2$$

The total surface area on water side is:

$$A_2 = A_{p,2} + A_{f,2}$$

$$= (43409.055 \text{ mm}^2) + (849267.961 \text{ mm}^2) = 892677.512 \text{ mm}^2$$

The free flow area on water side is given by the frontal area on water side minus the area blocked by the fins at the entrance of the core on that side:

$$A_{0,2} = b_2 \cdot L_1 \cdot (N_p + 1) - [(b_2 - \delta) + p_f] \cdot \delta \cdot n_f$$

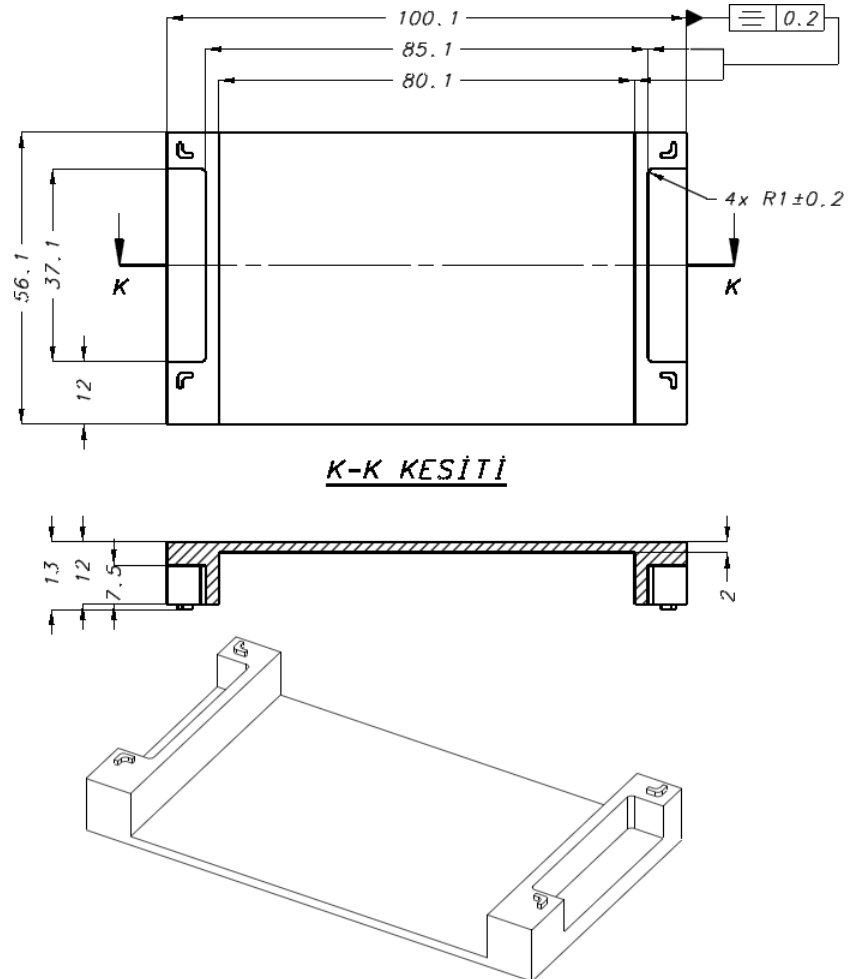
$$= (10 \text{ mm}) \cdot (85 \text{ mm}) \cdot (7) - [(10 \text{ mm} - 0.2 \text{ mm}) + 0.55] \cdot (0.2 \text{ mm})$$


$$\cdot \left(46 \frac{\text{fin}}{25.4 \text{ mm}}\right) \cdot (85 \text{ mm}) \cdot (7)$$

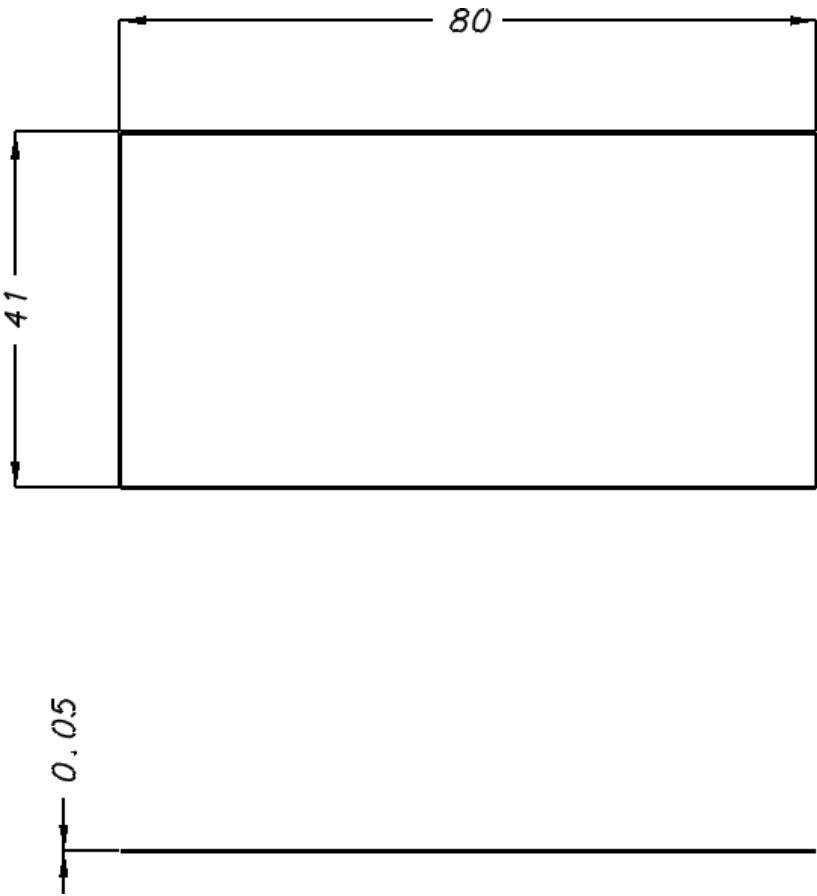
$$= 3719.453 \text{ mm}^2$$

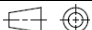
CHAPTER 5

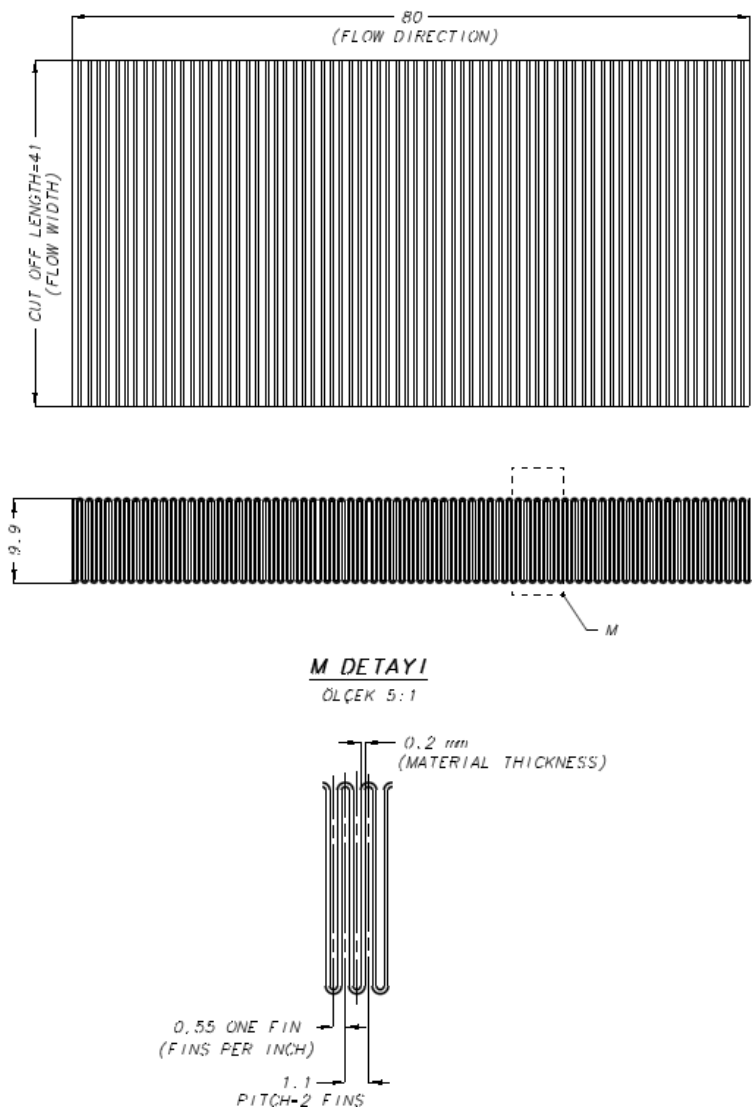
DRAWINGS OF THE MICROCHANNEL HEAT EXCHANGER



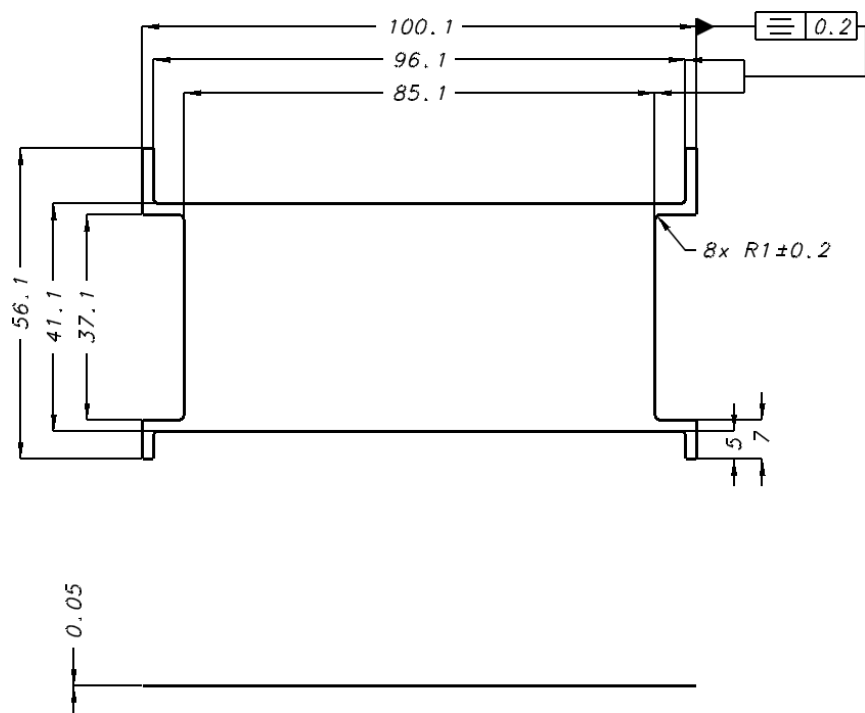
1		BASE PLATE			
Part number		Part description			
Scale	Unit	General Roughness	Tolerances unless otherwise stated	Material	Burr free
1:1	mm	3.2 \square m ✓	± 0.1 mm / ± 30 \square	AL 6061-T6	



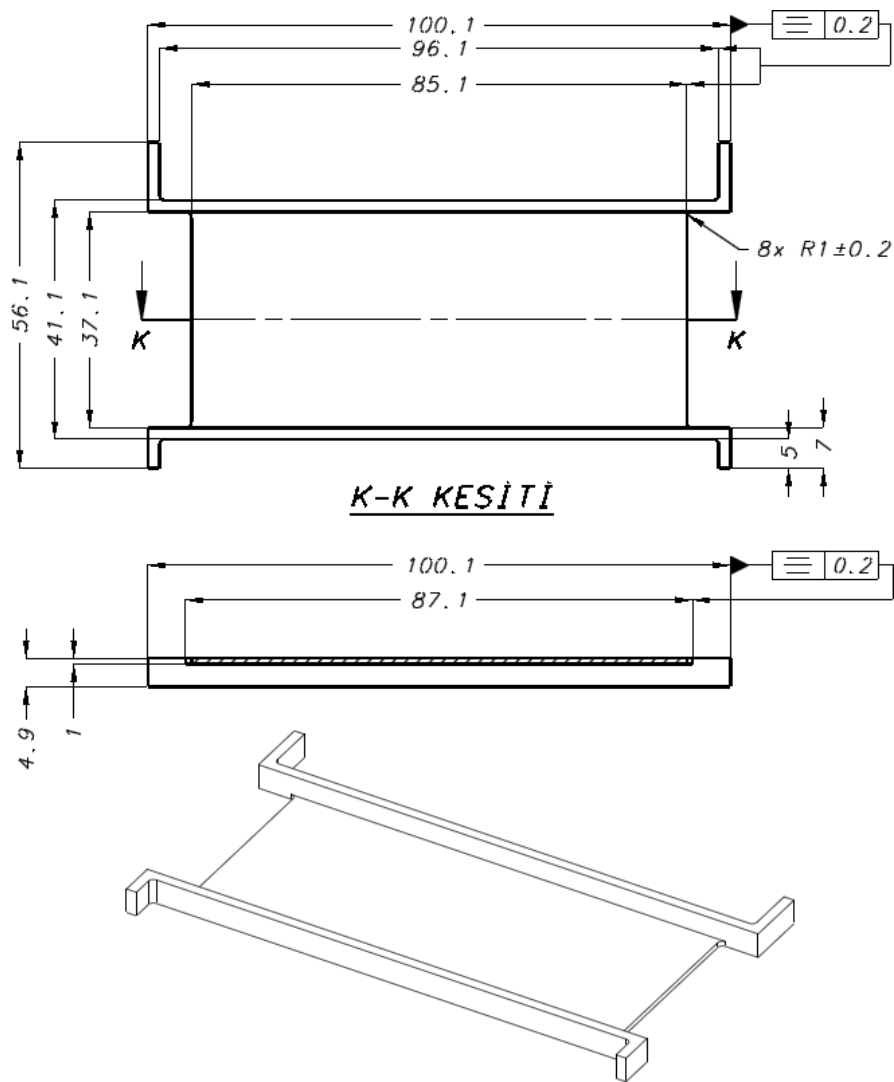
2		FOIL BASE PLATE SIDE			
Part number		Part description			
Scale	Unit	General Roughness	Tolerances unless otherwise stated	Material	Burr free
1:1	mm	3.2 \square m \checkmark	± 0.1 mm / ± 30 \square	AL 4004	

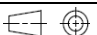


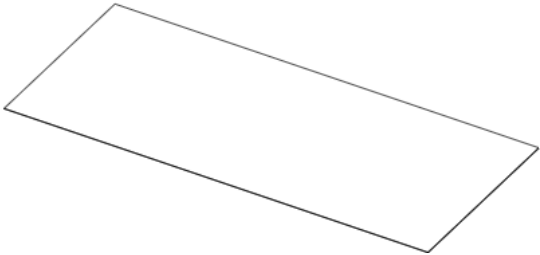
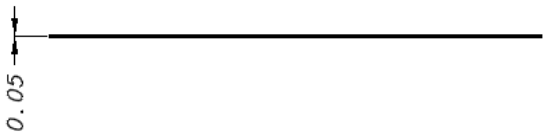
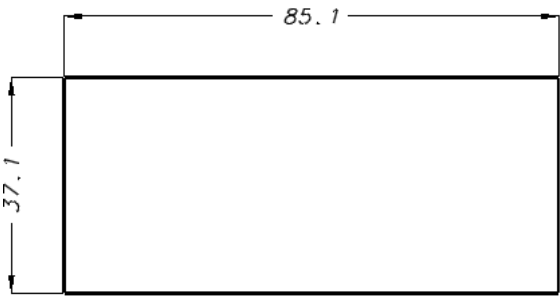
3		FIN AIR SIDE			
Part number		Part description			
Scale	Unit	General Roughness	Tolerances unless otherwise stated	Material	Burr free
1:1	mm	3.2 \square m \checkmark	± 0.1 mm / ± 30 \square	AL 3003-O	




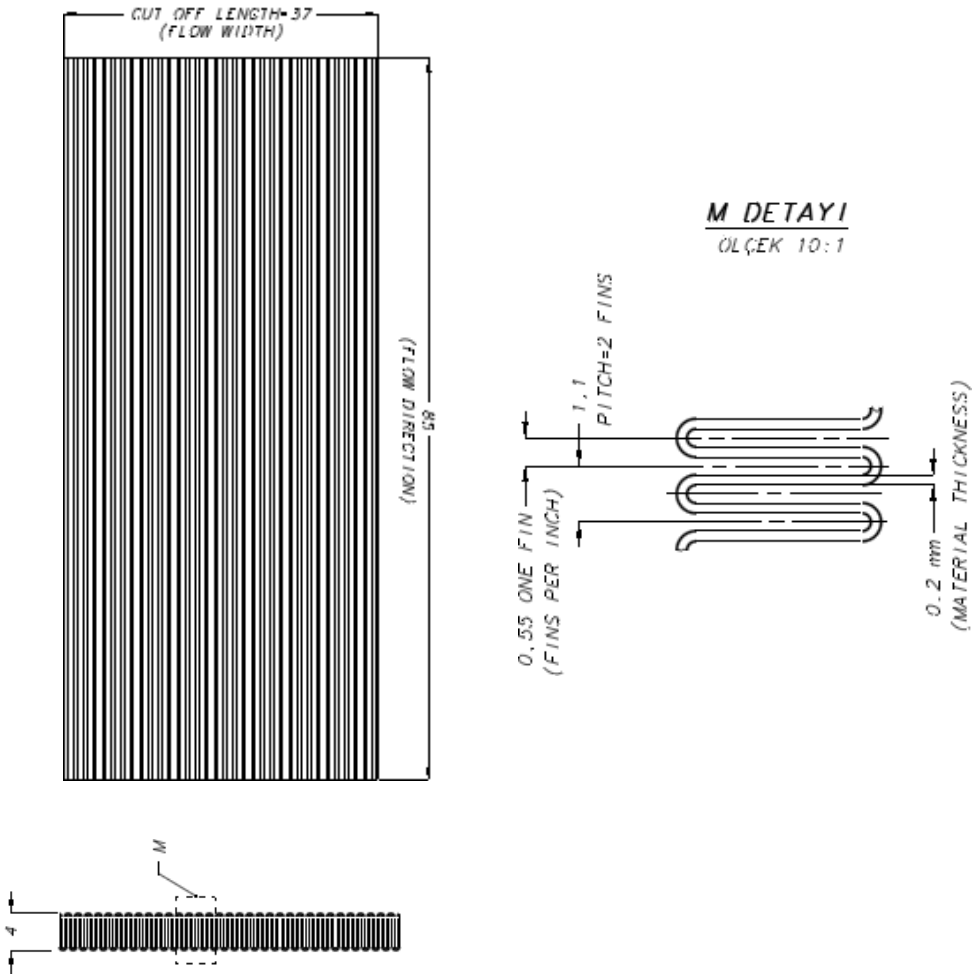
4		FOIL AIR-WATER SIDE			
Part number		Part description			
Scale	Unit	General Roughness	Tolerances unless otherwise stated	Material	Burr free
1:1	mm	3.2 \square m \checkmark	± 0.1 mm / ± 30 \square	AL 4004	

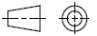


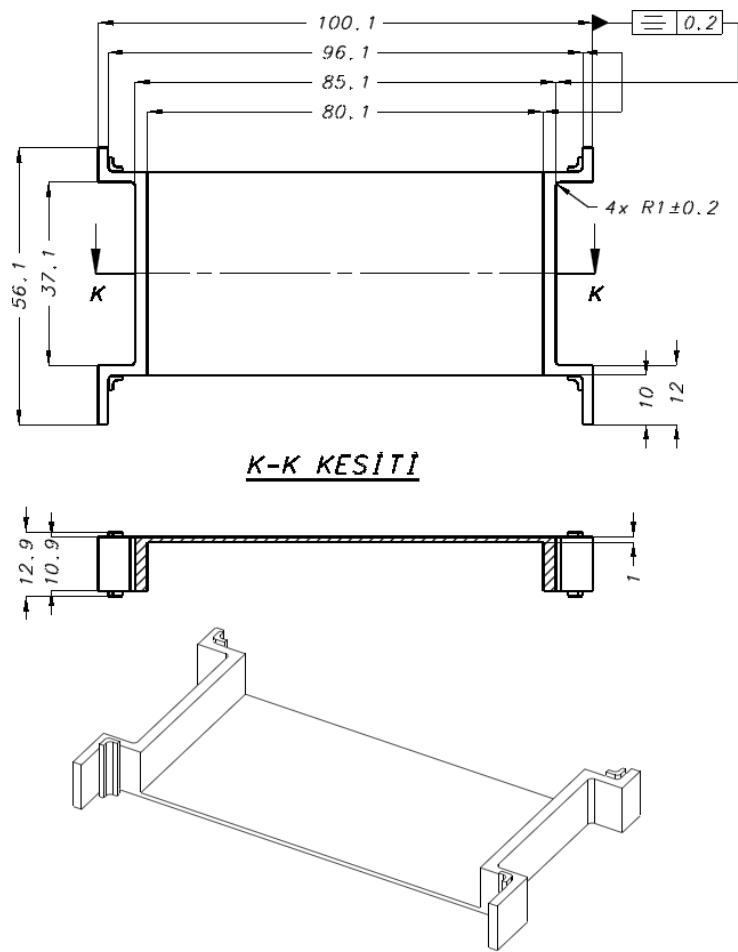
5		WATER BASE PLATE			
Part number		Part description			
Scale	Unit	General Roughness	Tolerances unless otherwise stated	Material	Burr free
1:1	mm	3.2 \square m \checkmark	± 0.1 mm / ± 30 \square	AL 6061-T6	



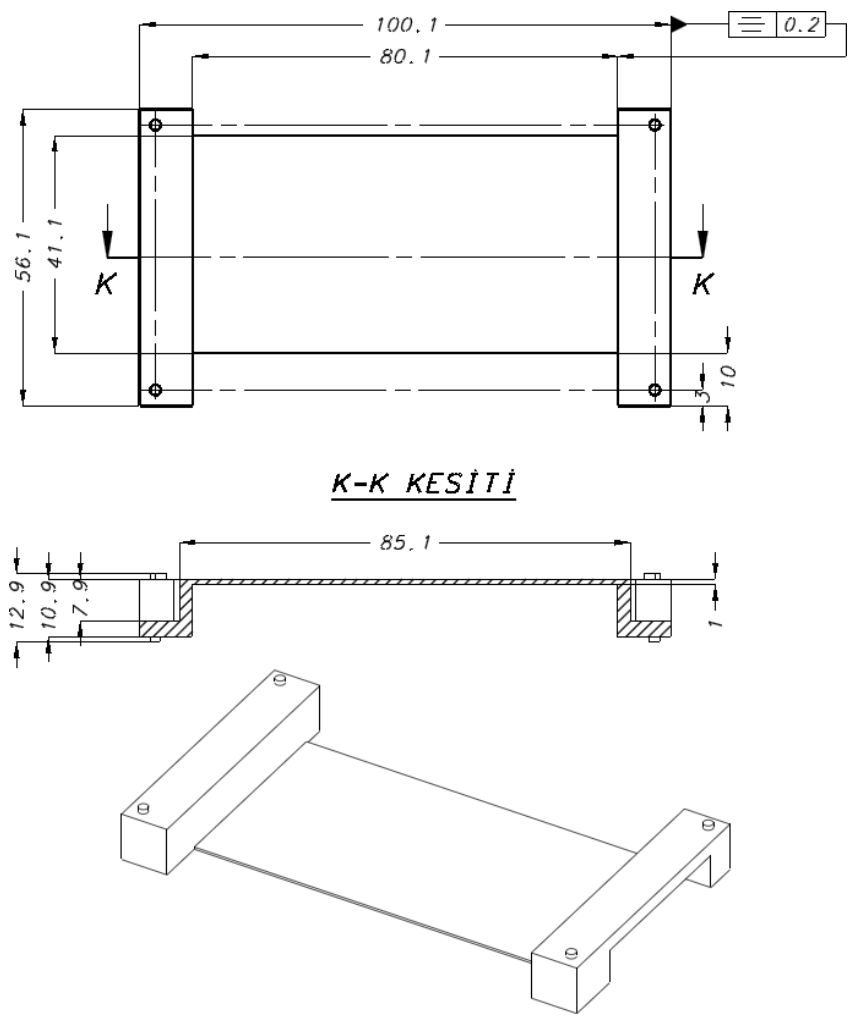
6		FOIL WATER SIDE			
Part number		Part description			
Scale	Unit	General Roughness	Tolerances unless otherwise stated	Material	Burr free
1:1	mm	3.2 \square m \checkmark	± 0.1 mm / ± 30 \square	AL 4004	

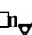
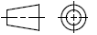


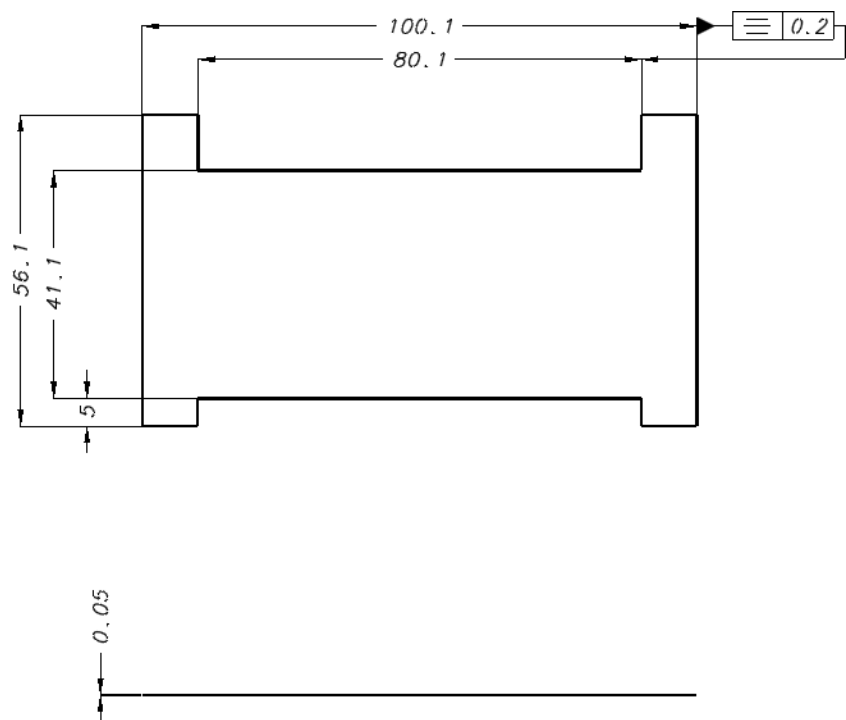
7		FIN WATER SIDE			
Part number		Part description			
Scale	Unit	General Roughness	Tolerances unless otherwise stated	Material	Burr free
1:1	mm	3.2 \square m \checkmark	± 0.1 mm / ± 30 \square	AL 3003-O	




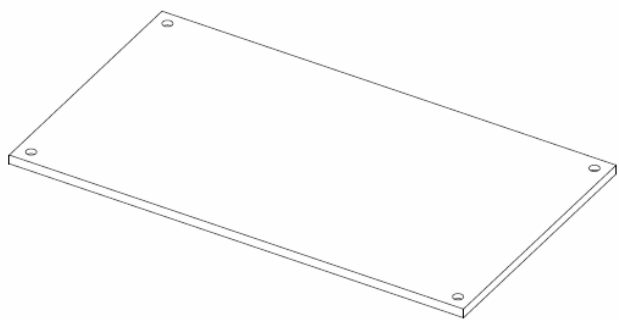
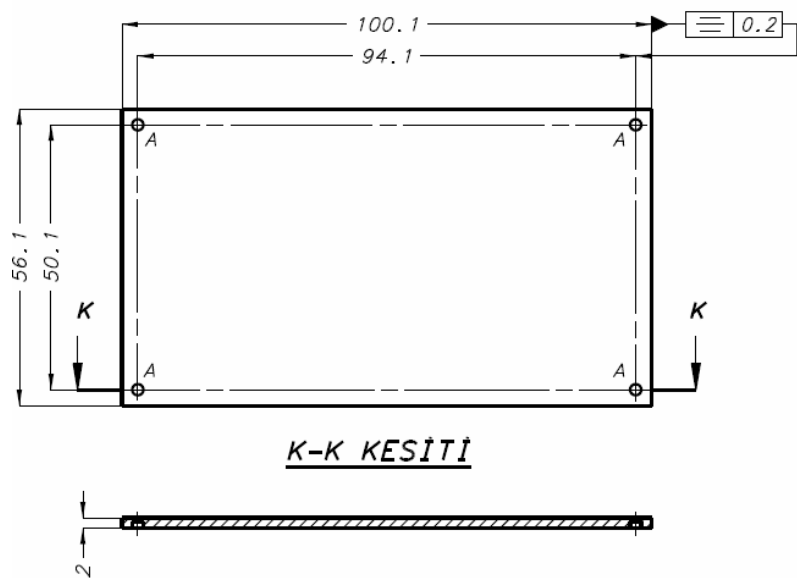
8		AIR BASE PLATE			
Part number		Part description			
Scale	Unit	General Roughness	Tolerances unless otherwise stated	Material	Burr free
1:1	mm	3.2 \square m \checkmark	± 0.1 mm / ± 30 \square	AL 6061-T6	




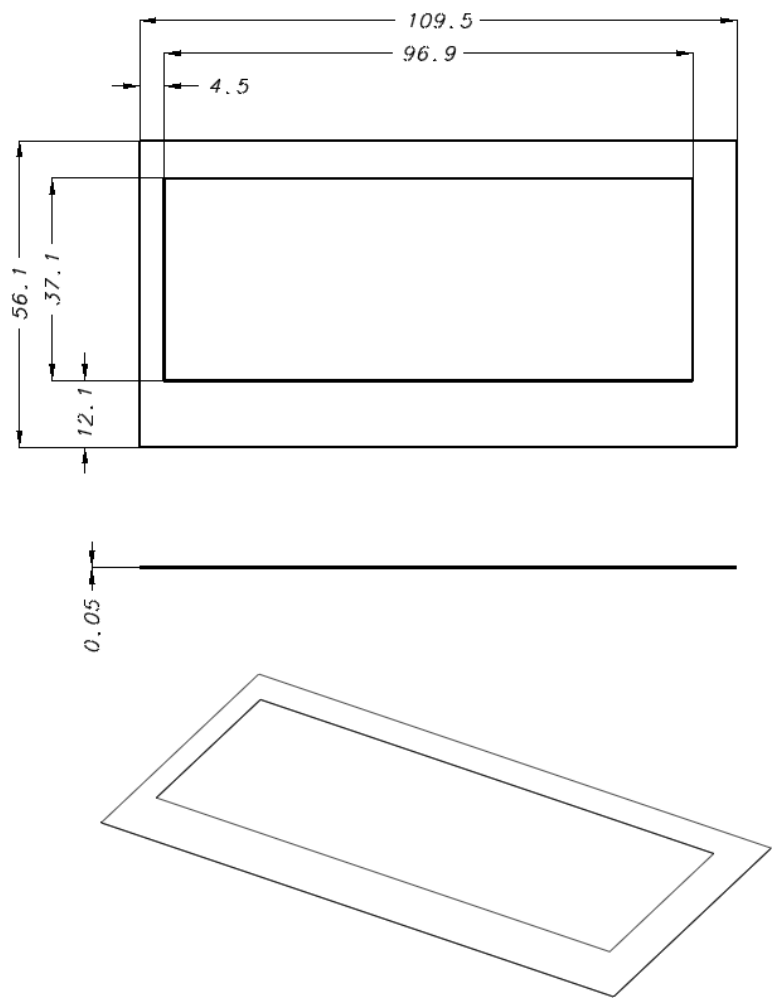
9		TOP AIR PLATE			
Part number		Part description			
Scale	Unit	General Roughness	Tolerances unless otherwise stated	Material	Burr free
1:1	mm	3.2 	$\pm 0.1 \text{ mm} / \pm 30 \text{ } \square$	AL 6061-T6	




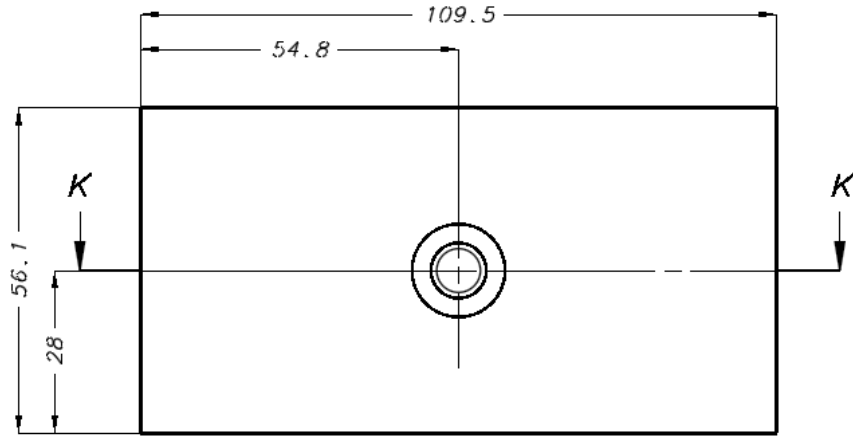
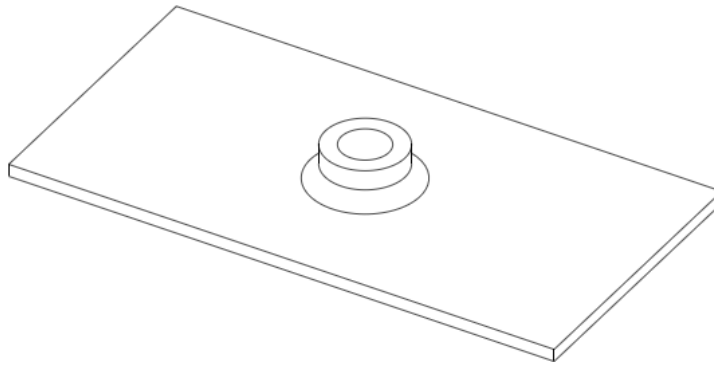
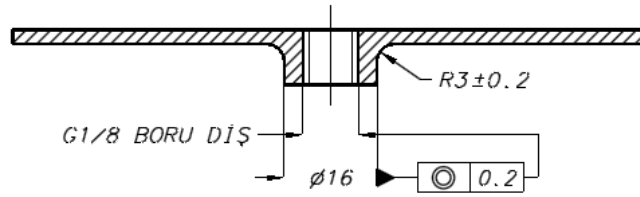
10		FOIL TOP PLATE SIDE			
Part number		Part description			
Scale	Unit	General Roughness	Tolerances unless otherwise stated	Material	Burr free
1:1	mm	3.2 $\sqrt{\text{m}}$ ✓	$\pm 0.1 \text{ mm} / \pm 30 \text{ } \square$	AL 4004	



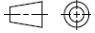
11		TOP PLATE			
Part number		Part description			
Scale	Unit	General Roughness	Tolerances unless otherwise stated	Material	Burr free
1:1	mm	3.2 \square m \checkmark	± 0.1 mm / ± 30 \square	AL 6061-T6	

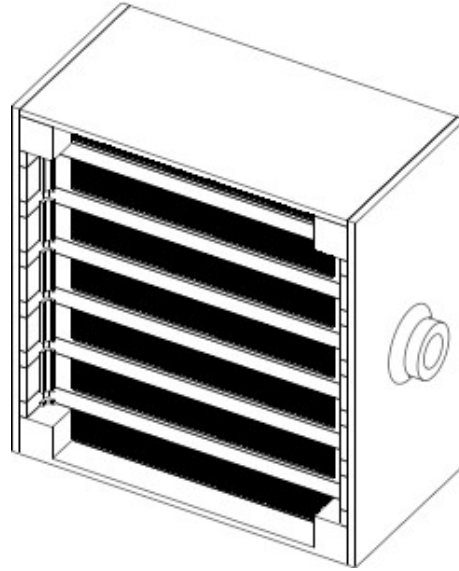


12		FOIL SIDE			
Part number		Part description			
Scale	Unit	General Roughness	Tolerances unless otherwise stated	Material	Burr free
1:1	mm	3.2 \square m \checkmark	± 0.1 mm / ± 30 \square	AL 4004	

**K-K KESİTİ**

13		SIDE PLATE			
Part number		Part description			
Scale	Unit	General Roughness	Tolerances unless otherwise stated	Material	Burr free

1:1	mm	3.2 \square m ✓	± 0.1 mm / ± 30 \square	AL 6061-T6	
-----	----	-------------------	-----------------------------------	------------	---



13	SIDE PLATE	2
12	FOIL SIDE	2
11	TOP PLATE	1
10	FOIL TOP PLATE SIDE	1
9	TOP AIR PLATE	1
8	AIR BASE PLATE	5
7	FIN WATER SIDE	6
6	FOIL WATER SIDE	6
5	WATER BASE PLATE	6
4	FOIL AIR-WATER SIDE	12
3	FIN AIR SIDE	7
2	FOIL BASE PLATE SIDE	7
1	BASE PLATE	1
Part Number	Part Description	Quantity

CHAPTER 6

Advantages and Disadvantages Microchannel Heat Exchanger

Advantages:

1.High Heat Transfer Ratios

The method used to manufacture the microchannel heat exchangers (brazed assembly). The contact between the tubes and fins of a traditional finned tube heat exchanger is mechanical, while the manufacture of the microchannel heat exchanger involves brazing, which provides the metallurgical bond between tubes and fins, eliminates contact resistance, and thus ensures higher heat transfer.

2.Low Airside Pressure Drops

Low airside resistance is yet another significant benefit of microchannel heat exchangers compared with traditional HVAC coil designs. If we compare a microchannel heat exchanger with a 6-row finned tube heat exchanger of similar size and capacity, the microchannel heat exchanger demonstrates 60% less airside pressure drop and therefore reduces fan power consumption as well as noise level produced by the fans. Thanks to the low resistance it is possible to increase airflow through a microchannel heat exchanger in order to increase the capacity of the cooling system.

3.Close Approach Temperatures

The same features that give the microchannel heat exchanger its high efficiency also makes it possible to reach close approach temperatures between the air and refrigerant which is particularly important in HVAC applications.

4.Smaller Sizes, Compact Design

Microchannel heat exchangers with 32-mm tube width provide the almost equal performance as 6-row finned tube heat exchanger with the same face area. To replace a traditional heat exchanger with the lower number of rows, a smaller and therefore less costly microchannel heat exchanger can be used. Depending on the application, this may also permit to increase the heat exchanging surface, leading to unprecedented increases in performance and/or energy efficiency of the HVAC system.

5. Robust Construction

In contrast to traditional finned tube heat exchangers, the core of a microchannel heat exchanger is extremely robust; the fins of microchannel heat exchangers are well protected from bending and mechanical damaging.

6. Low Weight

The low weight, compact size and reduced internal volume of an all-aluminum microchannel heat exchanger were key factors in its dramatic increase in popularity in the automobile industry. These characteristics are significant indeed and in the field of cooling systems, especially when it comes to mobile cooling systems. Their reduced size and weight lead not only to the lower transport and handling costs but also to the reduced cost of labor.

7. Lower Equipment Cost

The above-mentioned advantages of microchannel heat exchangers have led to a reduction in the overall cost of the equipment, which benefits from smaller heat exchanger size, reduced refrigerant charges, use of smaller fans, and a reduction in the number of parts used in the construction. It must be also noted that the cooling units based on microchannel heat exchangers allow elimination of some elements from; for instance, direct expansion systems do not require a refrigerant distributor anymore, a component that is both fragile and expensive in terms of labor cost.

Experience shows that the end cost of equipment that uses microchannel heat exchangers is at least 10% lower than that of equipment based on traditional heat exchangers.

Disadvantages:

- High pressure losses due to small size; requires use of high pressure.
- High price resulting in limited use.
- Limited knowledge involving engineering methods at this scale.

CHAPTER 7

Applications of Microchannel Heat Exchanger

- **Microchannel heat exchangers** have applications in several important and diverse fields including: aerospace; automotive; bioengineering; cooling of gas turbine blades, power and process industries; refrigeration and air conditioning; infrared detectors and powerful laser mirrors and superconductors; microelectronics.
- Micro-channel heat exchangers have been extensively used in automotive air conditioning systems but never been used in residential air-conditioners. Hence researchers first studied the automobile air conditioners.
- The geometry of inlet and outlet manifolds which are responsible for distributing and gathering of fluid in channels is an important factor for designing microfluidic heat exchangers.
- Thermal resistance off low in a tube or over a plate mainly concentrates in the thermal boundary layer. Therefore, a small thermal resistance is expected due to an extremely small thermal boundary layer in the microchannel. Heat transfer and friction in microchannel have received a considerable attention in recent years. Experimental studies are performed on gases, liquids, and two phase boiling.
- Based on the results from the above studies, the general features of heat transfer and flow friction of micro channels can be summarized as follows:

1. Conversion from laminar to transition regimes occurs at much smaller Reynolds numbers, and the transition region is limited in a smaller Reynolds number zone than for conventional channels.

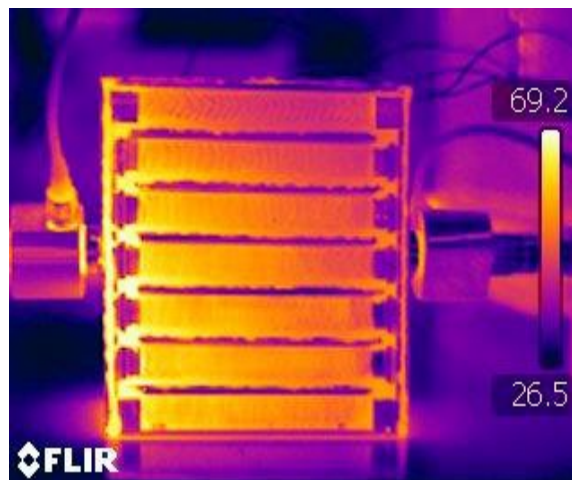
2. The friction and heat transfer correlations often deviate from the conventional one for large tubes.

3. The geometric parameters of microchannel, especially the hydraulic diameter and the aspect ratio of the channel, have critical effects not only on the flow transition Reynolds number but also on the friction factor and the heat transfer coefficient. As the characteristic diameter approaches the molecular or substructure level, an analysis based on the classical continuum.

CONCLUSION

Heat dissipation becomes a major problem in military systems. Heat exchangers are significant parts of these systems. Microchannel provide high heat transfer coefficients because of their small hydraulic diameters. Since high heat fluxes have to be removed from military systems, the structure of the heat exchanger was selected as microchannel. Then, available plain fins, whose heights were 4 mm and 10 mm, were used to form the microchannel structure of the heat exchanger.

Although the present study has produced satisfactory results as a pioneering study in the field of microchannel heat exchanger in Turkey, much additional work is required to reach state-of-the art quality.



It is observed that the surface temperature of microchannel heat exchanger changes rather much from left upper corner of microchannel heat exchanger to right bottom corner of microchannel heat exchanger.

In other words, almost half of microchannel heat exchanger is not used to heat transfer as effectively as the other half of the microchannel heat exchanger.

Due to manufacturing restrictions in vacuum brazing, the microchannel heat exchanger was produced with six rows for water flow.

Therefore, water almost does not pass through the upper three rows. In the future, the microchannel heat exchanger has to be redesigned with less rows and so that the microchannel is a two pass heat exchanger.

In redesigned microchannel heat exchanger, upper rows may be used for entering water and after one pass of water, lower rows may be used for exit the water. As water passes twice, air may be cooled much more effectively. This will result in a decrease of the outlet temperature of water and an increase in the effectiveness of microchannel heat exchanger.

To increase surface area on both sides, offset strip fins may be used. Therefore, turbulent flow may be achieved to increase heat transfer rate from water to air. Geometrical dimensions can be determined according to fan outside dimensions. In this way usage of surface area will be increased and non-used surface area will decrease.

REFERENCES

- [1] R. K. Shah and D. P. Sekulic, Fundamentals of Heat Exchanger Design, John Wiley & Sons

- [2] S. Kakaç and H. Liu, Heat Exchangers Selection, Rating and Thermal Design, 2nd Edition, CRC Press LLC

- [3] S. Kakaç, A.E. Bergles, F. Mayinger, Heat Exchangers Thermal-Hydraulic Fundamentals and Design, Hemisphere Publishing Corporation

- [4] S. G. Kandlikar, S. Garimella, D. Li, S. Colin and M. R. King, Heat Transfer and Fluid Flow in Minichannels and Microchannel, Elsevier

- [5] F. P. Incropera and D. P. DeWitt, Fundamentals of Heat and Mass Transfer, 4th Edition, John Wiley & Sons